

Improving a land surface scheme for estimating sensible and latent heat fluxes above grasslands with contrasting soil moisture zones

Kazeem A. Ishola^{a,b,d,*}, Gerald Mills^c, Reamonn M. Fealy^d, Órlaith Ní Choncubhair^e, Rowan Fealy^{a,b}

^a Irish Climate Analysis and Research Units (ICARUS), Maynooth University, Ireland

^b Department of Geography, Maynooth University, Co. Kildare, Ireland

^c School of Geography, University College Dublin, Co. Dublin, Ireland

^d Teagasc Agrifood Business and Spatial Analysis Department, Ashtown, Co. Dublin, Ireland

^e Teagasc Environmental Research Centre, Johnstown Castle, Co. Wexford, Ireland

ARTICLE INFO

Keywords:

Surface resistance
Surface-atmosphere exchange
Surface-layer schemes
Agriculture

ABSTRACT

Knowledge of soil–vegetation–atmosphere energy exchange processes is essential for examining the response of agriculture to changes in climate in both the short and long term. However, there are relatively few sites where all the flux measurements necessary for evaluating these responses are available; where they exist, data are often incomplete and/or of limited duration. At the same time, there is often an extensive observation network available that has gathered key meteorological data (sunshine, wind, rainfall, etc.) over decades. Simulating the terms of the surface energy balance (SEB) using available meteorological, soil and vegetation data can improve our understanding of how agricultural systems respond to climate and how this response will vary spatially. Here, we employ a physically-based scheme to simulate the SEB fluxes over a mid-latitude, maritime temperate environment using routine weather observations. The latent heat flux is a critical SEB term as it incorporates the response of the plant to environmental conditions including available energy and soil water. This response is represented in modeling schemes through surface resistance (r_s), which is usually expressed as a function of near-surface water vapor alone. In this study, we simulate the SEB over two grassland sites, where eddy flux observations are available, representing imperfectly- and poorly- drained soils. We employ three different formulations of r_s , representing varying degrees of sophistication, to estimate the surface fluxes. Due to differences in soil moisture characteristics between the sites, we ultimately focused our attention on an r_s formulation that accounted for soil water retention capacity, based on the Jarvis conductance model; the results at both hourly and daily intervals are in good agreement, with RMSE values of $\approx 40 \text{ W m}^{-2}$ for sensible and latent heat fluxes at both sites. The findings show the potential value of using routine weather observations to generate the SEB where flux observations are not available and the importance of soil properties in estimating surface fluxes. These findings could contribute to the assessment of past and future climate change on grassland ecosystems.

1. Introduction

Information on the exchange of heat and moisture at the Earth's surface is needed to evaluate the performance of climate models in simulating land-atmosphere interactions (e.g. Knist et al., 2017) and for applications in a number of areas, such as agricultural productivity, soil moisture and hydrology, boundary-layer development, etc. (de Bruin et al., 1993; van den Hurk et al., 2000; Chen and Dudhia, 2001; Jung et al., 2010; Lathuilliere et al., 2012; van de Boer et al., 2013, 2014b). Typically, these exchanges are expressed in terms of the surface energy balance (SEB, see Appendix 1) which stipulates that net

radiation (Q_N) is expended as sensible heat flux by conduction with the soil (Q_G) and as sensible (Q_H) and latent (Q_E) heat fluxes by turbulence with the overlying atmosphere. However, measurements of these flux densities are not routine practice, partly due to the complexity of turbulence measurement and the relative cost of instrumentation (Haymann et al., 2019). To overcome this challenge, past and recent studies have developed physically-based schemes to simulate these exchanges based on routine meteorological observations (de Bruin and Holtslag, 1982; Holtslag and van Ulden, 1983; Holtslag and de Bruin, 1988; Viterbo and Beljaars, 1995; Chen et al., 1996; Beljaars and Bosveld, 1997; Mohan and Siddiqui, 1998; de Rooy and Holtslag, 1999;

* Corresponding author at: Irish Climate Analysis and Research Units (ICARUS), Maynooth University, Ireland.

E-mail address: kazeem.ishola.2018@mumail.ie (K.A. Ishola).

Nomenclature

A_g	soil heat transfer coefficient ($\text{W m}^{-2} \text{K}^{-1}$)	r_a	aerodynamic resistance (s m^{-1})
c_p	specific heat capacity of air ($\text{J kg}^{-1} \text{K}^{-1}$)	r_s	the surface resistance (s m^{-1})
c_{soil}	soil moisture coefficient ($\text{m}^3 \text{m}^{-3}$).	$r_{s, min}$	minimum stomatal resistance (s m^{-1})
e	vapor pressure (kPa)	s	slope of saturated vapor pressure curves (kPa K^{-1})
F_M	soil moisture stress function	S_r	global radiation coefficient (W m^{-2})
F_S	solar radiation stress function	T_a	air temperature at z_a (K)
$F_{\Delta q}$	air moisture deficit function	T_s	surface temperature (K)
F_T	near-surface temperature function	T_{24}	24-h moving average of T_a (K)
f_r	an empirical site-specific constant	u	wind speed at 10 m (m s^{-1})
g	acceleration due to gravity (m s^{-2})	u_*	friction velocity (m s^{-1})
h_s	moisture deficit coefficient (kg kg^{-1})	z_a	observation height, 2 m.
k	von Kàrmàn constant	z_{oH}	surface roughness length for heat (m)
L	Obukhov length (m)	z_{om}	surface roughness length for momentum (m)
LAI	leaf area index ($\text{m}^2 \text{m}^{-2}$)	α	surface albedo
N	cloud amount (oktas)	γ	psychrometric constant (kPa K^{-1})
P	mean sea level pressure (kPa)	Γ_d	dry adiabatic lapse rate (K m^{-1})
Q_E	latent heat flux (W m^{-2})	Δq_a	specific humidity deficit at z_a (kg kg^{-1}).
Q_G	soil heat flux (W m^{-2})	Δq_s	specific humidity deficit at the surface (kg kg^{-1})
Q_H	sensible heat flux (W m^{-2})	ε	surface emissivity
Q_N	net radiation (W m^{-2})	ε_a	atmospheric emissivity
$Q_{L\downarrow}$	incoming longwave radiation (W m^{-2})	θ	volumetric soil moisture in the root zone ($\text{m}^3 \text{m}^{-3}$)
$Q_{L\uparrow}$	outgoing longwave radiation (W m^{-2})	θ_{CT}	critical soil moisture ($\text{m}^3 \text{m}^{-3}$)
$Q_{S\downarrow}$	global solar radiation (W m^{-2})	θ_{FC}	field capacity ($\text{m}^3 \text{m}^{-3}$)
$Q_{S\uparrow}$	outgoing shortwave radiation (W m^{-2})	θ_{ST}	saturation point ($\text{m}^3 \text{m}^{-3}$)
$Q_{\Delta S}$	soil heat storage (W m^{-2})	θ_{WP}	wilting point ($\text{m}^3 \text{m}^{-3}$)
RH	relative humidity (%)	θ_*	temperature scale (K)
R_d	specific gas constant for dry air ($\text{J kg}^{-1} \text{K}^{-1}$)	ρ	density of dry air (kg m^{-3})
R_v	specific gas constant for water vapor ($\text{J kg}^{-1} \text{K}^{-1}$)	σ	stefan Boltzmann's constant ($\text{W m}^{-2} \text{K}^{-1}$)
		ψ_H	dimensionless stability term for heat
		ψ_M	dimensionless stability term for momentum

van de Boer et al., 2014a; Lu et al., 2014). Although the choice of scheme is dependent on the availability of input meteorological parameters, the analytic context is usually based on the Monin–Obukhov Similarity Theory (MOST), which uses vertical profiles of air temperature, humidity and wind to simulate the fluxes of heat, vapor and momentum, respectively, within the atmospheric surface layer (Appendix 1). However, issues remain with these schemes. For example, Chen et al. (1997) found large discrepancies between schemes that have been partly attributed to the dependence on empirical constants derived from site specific data.

de Rooy and Holtslag (1999) proposed and evaluated a scheme for estimating SEB fluxes using a minimal number of input parameters derived from single-level routine weather observations. The methodology was developed based on observations made over short grass in Cabauw, the Netherlands, and has not been evaluated elsewhere. More recently, van de Boer et al. (2014a) proposed a modified version of this scheme which was evaluated at two locations over different land cover types. This modified scheme accounts for the dependency of each flux on air, rather than surface, temperature as in de Rooy and Holtslag (1999). In addition, it employs a modified formulation for surface resistance (r_s) a key parameter in the estimation of Q_E as it accounts for soil moisture content and the transfer of soil water to the atmosphere by evapotranspiration. There are different methods of parameterizing r_s (Kim and Verma, 1991; Jacobs, 1994) but one of the most widely used is that of Jarvis (1976), which incorporates environmental controls, including atmospheric (radiation, temperature, vapor pressure deficit, CO_2 concentration), vegetation (Leaf Area Index) and soil (soil water) factors (e.g. Stewart, 1988; Beljaars and Bosveld, 1997; Niyogi and Raman, 1997; de Rooy and Holtslag, 1999; van de Boer et al., 2014a). Where it is assumed that there is no moisture stress, the dependence of r_s on soil water content has either been excluded (van de Boer et al., 2014a) or assumed to be negligible (de Rooy and Holtslag, 1999). However, under conditions of increasing soil

moisture stress, water availability acts to regulate r_s (Russell, 1980; Sherratt and Wheeler, 1984) and consequently plays a prominent role in modulating heat and moisture fluxes (Sherratt and Wheeler, 1984; Betts and Ball, 1995; 1998; Senevirante et al., 2010). Increased r_s due to limited water availability affects evapotranspiration and is a major factor controlling the productivity of terrestrial ecosystems (Ciais et al., 2005; De Boeck et al., 2011; Reichstein et al., 2007; Teuling et al., 2006; Zhang et al., 2012). The parameterization of r_s has also been identified as playing a significant role in contributing to model uncertainties in estimating Q_E and gross primary production (GPP) in land surface models (Li et al., 2016).

In this study we examine the influence of available soil moisture on the simulation of energy fluxes using the de Rooy and Holtslag (1999) scheme. We identify two grassland sites in Ireland that have the same precipitation regime but are distinguished by their soil characteristics and are defined as imperfectly- and poorly- drained soils. Our primary objectives are to; (1) examine whether the de Rooy and Holtslag (1999) scheme is transferrable to Irish sites; (2) evaluate if meteorological data from one location can be employed to estimate the measured surface fluxes at a nearby location and; (3) evaluate the response of surface fluxes to three different parameterizations of surface resistance (r_s).

The study seeks to extend the value of flux estimates to places where such observations are not available and contribute to the improvement and applicability of land surface schemes over grassland ecosystems.

2. Data and methods

2.1. Background climate

The climate of Ireland is dominated by westerly airflow off the North Atlantic and consequently exhibits a maritime temperate climate (Peel et al., 2007). Based on the long term averages over the period from 1981 to 2010, Ireland typically experiences cool summers with

daily maximum ranging from 18 to 20 °C and mild winters (8 °C); minimum temperatures fall below 0 °C on approximately 40 (10) days per year at inland (coastal) areas. Annual average rainfall is just over 1200 mm, which is distributed nearly evenly throughout the year. The highest rainfall is typically recorded in upland regions on the west coast. Rainfall amounts decline moving eastwards, associated with airflow interactions with topography. However, topographic variations across the island are relatively small – the average elevation is 118 m a.s.l. and the highest peak is just over 1000 m a.s.l. A summary description of the climatology of the region is reported in Walsh (2012).

The climate in Ireland provides conditions suitable for the year-round grass growth, particularly along coastal margins in the south of the country which records a median grass growing season length of 330 days (Keane and Collins, 2004). Consequently, grassland land-cover is the most important crop and accounts for more than 90% of the land under agricultural production (McEniry et al., 2013) and 56% of the total land area (EUROSTAT, 2015). Due to the year-round precipitation, excessive soil moisture is generally more problematic for grass production than water deficits (McDonnell et al., 2018), particularly on poorly drained soils. However, soil moisture deficits are periodically experienced during the summer months, typically in the east and south east of the country (Dwyer and Walsh, 2012), associated with the

location of well drained soils (Fig. 1). In terms of soil characteristics, the General Soil Map of Ireland classifies the south-east as mostly free-draining sandy soils, with limestone-rich soils in the south and midlands, and acid and peat soils on mountains, hills and the western seaboard (Gardiner and Radford, 1980). More detailed soil properties combining previous and existing soil survey information for Ireland is available from Creamer et al. (2014).

2.2. Site descriptions

Two sites are employed in this study representing imperfectly drained (Johnstown Castle, Co. Wexford) and poorly drained (Dripsey, Co. Cork) soil characteristics; Table 1 provides summary information on each site and Fig. 1 shows the site locations. Both sites have available eddy covariance (EC) flux tower measurements.

Details on the vegetation and soil characteristics associated with the flux tower footprints are as follows:

- i) Johnstown Castle: Two main types of soil (Gleys and Brown Earths), have been reported within the flux site footprint (Peichl et al., 2012). The soil within the flux footprint (< 150 m) is moderately to imperfectly drained Gley (FAO classification: Gleyic Cambisol). The

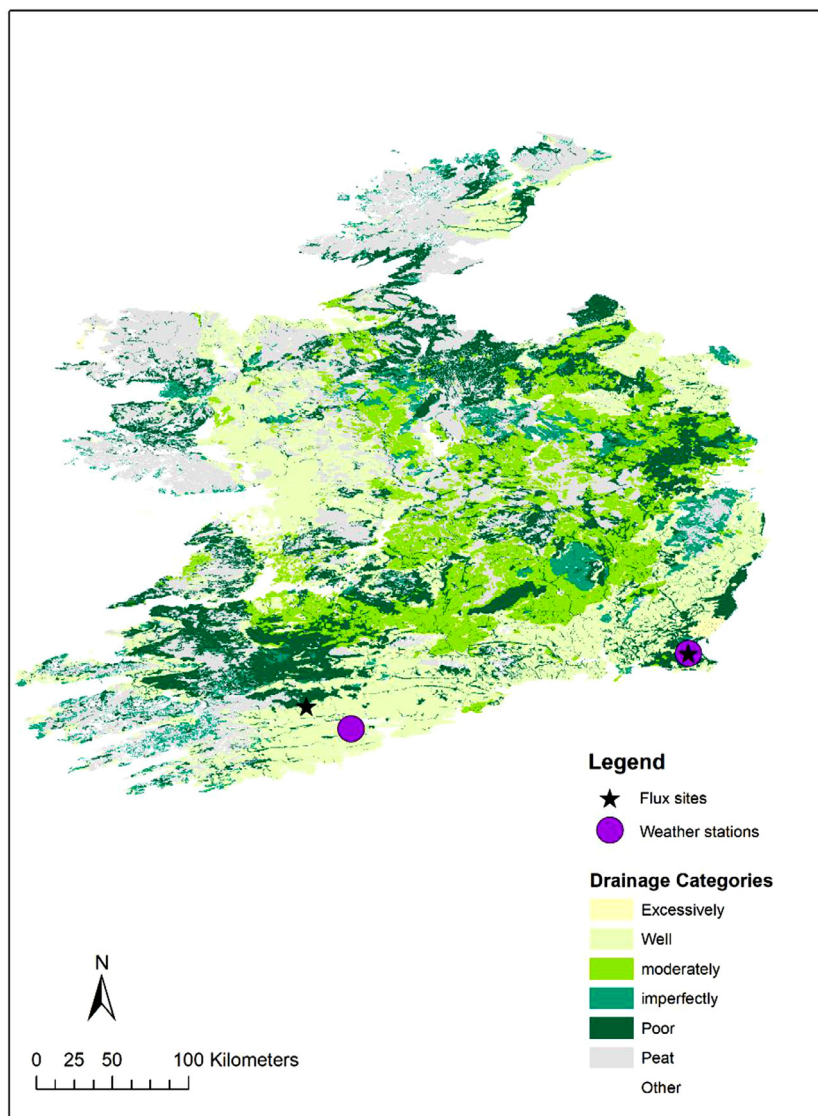


Fig 1. Map of soil drainage classes of Ireland (Irish Soil Information System by Teagasc for EPA, Creamer et al., 2014), showing the locations of test sites.

Table 1

Descriptions of grassland eddy covariance flux and synoptic stations used in this study. Meteorological data from Cork Airport (51.84°N, 8.48°W) at an elevation of 155 m were used for Dripsey. Johnstown Castle has a co-located weather station. The soil moisture properties are field capacity (θ_{FC}), saturation level (θ_{ST}) and wilting point (θ_{WP}), in order.

Station	Lat/Long (°)	Elevation (m)	Soil description	Moisture properties (θ_{FC} , θ_{ST} , θ_{WP})	Drainage class	Time period
Johnstown Castle	52.29°N, 6.49°W	58	A combination of gley, brown earths and free draining fine siliceous loam soils.	32% 59% 17%	Imperfect	2013
Dripsey	51.98°N, 8.75°W	186	Gley water-logged soils.	32% 45% 12%	Poor	2010

soils transition to moderately or well drained Brown Earths (Cambisol) at the outer edge of the flux footprint. The soil class in this area therefore varies from moderately to imperfectly drained, and the land cover is grass.

- ii) Dripsey: The EC footprint is over grass cover on a soil type that impedes water movement and can become waterlogged (Kiely et al., 2018) and is classed as a poorly drained Gley soil.

More detailed descriptions on the soil properties, climatology and EC footprints at Dripsey and Johnstown Castle are reported in Kiely et al. (2018) and Peichl et al. (2012), respectively.

Detailed information on vegetation height and leaf area index (LAI) are not available for the periods corresponding with flux measurements made at Dripsey, but Kiely et al. (2018) reported LAI values ranging from $\approx 2 \text{ m}^2 \text{ m}^{-2}$ in winter to $\approx 6 \text{ m}^2 \text{ m}^{-2}$ in summer. At Johnstown Castle, LAI is estimated from measurements of grass dry matter yield concurrent with the EC observations and an allometric relationship established with leaf area index meter readings. Modeled LAI values range between 0.1 (winter) and $6.8 \text{ m}^2 \text{ m}^{-2}$ (summer) for this site, with an average LAI of $2.2 \text{ m}^2 \text{ m}^{-2}$.

2.3. Data

We employ available routine weather observations to parameterize surface fluxes of heat and moisture over the two grassland sites described above. In the following sections, the observed flux data available for each site is discussed followed by a description of the available meteorological and soil water data. A summary of the Eddy-covariance and meteorological parameters used as input to, and evaluation of, the scheme employed is presented in Table 2.

2.3.1. Eddy-covariance measurements

Sensible and latent heat fluxes: Half-hourly EC flux measurements of Q_H and Q_E are available from the European Fluxes Database Cluster (<http://www.europe-fluxdata.eu/>) (Papale et al., 2006) for Dripsey (Kiely et al., 2018) for the period 2010. In order to avoid any potential

bias, we only employed non gap-filled data (Level 2 data). Half-hourly EC flux measurements of Q_H and Q_E were also obtained for Johnstown Castle for 2013 (Unpublished results). The instrumentation at both sites consists of an open-path infra-red gas analyser (IRGA) for measuring H_2O density and CO_2 concentration, in combination with a 3D sonic anemometer. The EC data were logged at 10 Hz and averaged over 30-minutes intervals (see Table 2 for a list of instruments at each site).

Data processing procedures at both sites were similar and are documented elsewhere: Sottocornola and Kiely (2010a, 2010b) for Dripsey; and Ní Choncubhair et al. (2017) for Johnstown Castle. These procedures include spike removal (Vickers and Mahrt, 1997), the Webb–Pearman–Leuning correction (Webb et al., 1980; Moncrieff et al., 1997a), sonic anemometer tilt correction using the double rotation method (Kaimal and Finnigan, 1994) and spectral attenuation corrections after Moncrieff et al. (1997b). Some data filtering procedures, which differ from the above approaches, were applied to Dripsey and are described in Kiely et al. (2018). Here, poor quality data based on quality control flags (QC = 2) were removed and flux observations recorded when precipitation exceeded 1 mm were removed as these are likely to generate errors in Q_E measurements using open-path sensors (e.g. Ma et al., 2015). A statistical examination of the processed data for all sites showed typical ranges of -100 – 400 W m^{-2} for Q_H and Q_E ; individual observations outside of these ranges were excluded from further analysis (following Ma et al., 2015).

Following these pre-processing steps, a significant percent (original plus filtered) of flux data at each site was classed as missing: 24% and 32% of Q_H and Q_E , respectively at Johnstown Castle and 28% and 31% of Q_H and Q_E at Dripsey. While the proportion of data gaps from Johnstown Castle mainly arose from the quality control procedures, the higher proportion of missing data from Dripsey was due to a combination of both the number of missing values in the original data and the quality control processes, outlined above. After the filtering processes, the proportion of nighttime data slightly exceeded the daytime data at both sites. At Johnstown Castle, approximately 51% (2941 h) and 49% (2939 h) of Q_E data remained for nighttime and daytime (08:00–18:00) hours, respectively. Similarly, 53% (3188 h) and 47% (2851 h) of data

Table 2

Descriptions of meteorology and eddy-covariance parameters used as forcings and for validation, respectively.

Variables	Usage		Instrumentation
	Forcing	Validation	
Q_N		x	NR-Lite (Johnstown) and CNR1 (Dripsey) (Kipp & Zonen, Delft, The Netherlands)
Q_{S1}	x		
T_a	x		
u	x		
P	x		
RH	x		
Precipitation			
Sunshine hours			
Q_{Hb} , Q_{Eb}		x	IRGA gas analyzers, LI-7500 (LI-COR, Lincoln, NE) at 6 m for Dripsey and; 2.28 m (1 st Jan. – 26 th Feb.), 2.72 m (26 th Feb. – 23 rd Oct.), 2.85 m (23 rd Oct. – 31 st Dec.) for Johnstown.
θ	x		CS616 (Johnstown) and CS615 (Dripsey) (Campbell Scientific, Shepherd, UK)

for Dripsey were available for analysis.

Net radiation: Half-hourly measurements of Q_N from Dripsey for 2010 are available from the European Fluxes Database Cluster (Papale et al., 2006). For Johnstown Castle, Q_N measurements for 2013 are available from previously unpublished research (see Section 2.3.1). Hourly values of Q_N in the range -100 and 700 W m^{-2} were selected for the subsequent analysis (following Shi and Liang, 2014).

The energy budget closure is an efficient approach to evaluate the consistency of scalar flux densities measured by EC systems (Twine et al., 2000). The approach relates available energy ($Q_N - Q_G$) to turbulent fluxes ($Q_H + Q_E$) in order to determine the magnitude of non-closure of measured fluxes by EC systems. EC measurements are known to underestimate the turbulent fluxes (Q_H and Q_E) and overestimate Q_N resulting in non-closure of the energy balance (EBC) (Wilson et al., 2002; Foken, 2008; Franssen et al., 2010; Stoy et al., 2013). Other potential reasons for non-closure are discussed extensively in the literature and include; the failure to measure heat storage terms as part of measurement programmes (e.g. Heusinkveld et al., 2004); large-scale turbulent circulations over heterogeneous landscapes that are not captured by EC methods (Mauder et al., 2007; Stoy et al., 2013); the assumption of no advection and; inaccurate Q_N measurements (e.g. Foken, 2008). Over the sites available for the present study, the hourly energy budget closure (ignoring the Q_G and Q_{AS} terms) is approximately 69 % at Johnstown Castle and 60% at Dripsey (Fig. 2). These closure values are comparable with previously reported values, which lie within 53 – 99 % (e.g. Wilson et al., 2002).

2.3.2. Meteorological data

On-site hourly meteorological observations for the same period of EC measurements are available for Johnstown Castle but at Dripsey these data are only available at Cork Airport (155 m a.s.l), which is approximately 25 km from the site. Both meteorological stations conform to World Meteorological Organization (WMO) guidelines and report on global solar radiation ($Q_{s\downarrow}$, W m^{-2}) or sun duration (hours), air temperature ($^{\circ}\text{C}$), relative humidity (%), pressure (kPa), wind speed (m s^{-1}) and precipitation (mm). As cloud amount (oktas) was only available from Cork Airport, it was excluded from the subsequent analysis; this value was set ≈ 0 in the calculation of $Q_{L\downarrow}$. Global solar radiation was not available from Cork Airport, therefore hourly $Q_{s\downarrow}$ data was estimated for this site based on observations of sunshine duration following Allen et al. (1998) and Ishola et al. (2018). The hourly meteorological observations correspond with the periods for which the flux data are available at the two sites.

2.3.3. Soil water data

Soil water content, measured as the volumetric water content (θ , $\text{m}^3 \text{ m}^{-3}$) in the upper 20 cm of the soil, was measured at both sites at half-hourly intervals using CS615/CS616 time domain reflectometers (Table 2). At Johnstown Castle, these measurements are contemporaneous with the available EC flux measurements. At Dripsey,

measurements are only available for 2004 and 2005, which coincides with periods when flux measurements are either not available or gap-filled (European Fluxes Database Cluster Level 3 and 4 data). While the general meteorological conditions at Dripsey during 2004 and 2005 were wetter than those experienced in 2010 (1174 mm; 1183 mm and 974 mm, respectively), the cumulative precipitation during 2005 was very similar in profile to 2010, up to October, after which the soils would have been close to or at field capacity.

2.4. Methods

2.4.1. Surface flux estimation

The scheme to estimate the fluxes of heat, moisture and momentum from limited routine weather data was adapted from de Rooy and Holtslag (1999). The scheme was originally developed over a grassland ecosystem using extensive and well-documented datasets from Cabauw, the Netherlands, and covering a variety of weather conditions. The scheme computes the turbulent fluxes (Q_H and Q_E) through a set of sequential calculations (Fig. 3). The required inputs are: air temperature T_a (K) at observation height z_a (2 m), relative humidity RH (%), wind speed u (m s^{-1}) at 10 m, mean sea level pressure P (kPa), global solar radiation $Q_{s\downarrow}$ (W m^{-2}) and cloud amount N (oktas).

In the initial step, the variables that can be obtained directly from the inputs, such as the 24-h mean of 2-m temperature, T_{24} (K), vapor pressure, e (kPa), specific humidity deficit, Δq_a (g kg^{-1}), psychrometric constant, γ (kPa K^{-1}), and the slope of the saturated vapor pressure curve, s (kPa K^{-1}), are estimated. An iterative procedure then estimates the following parameters: friction velocity, u_* (m s^{-1}), aerodynamic resistance, r_a ($\text{s}^{-1} \text{ m}$), Q_H (W m^{-2}), and subsequently temperature scale θ_* (K) and Obukhov length L (m), using flux profile relations (Paulson, 1970). The profile method adopts the MOST to describe the profile relationships of important scaling quantities, u_* , θ_* and L ; r_a is also expressed in terms of a flux-profile relationship. In this study, the empirical stability correction functions used in the profile method are based on those derived for unstable surface layer by Paulson (1970) and Dyer (1974), which relate the fluxes of heat and momentum to their non-dimensional vertical gradients.

The friction velocity, u_* , aerodynamic resistance r_a and sensible heat, Q_H are calculated as follows:

$$u_* = \frac{uk}{\left[\ln\left(\frac{z_a}{z_{om}}\right) - \psi_m\left(\frac{z_a}{L}\right) + \psi_m\left(\frac{z_{om}}{L}\right) \right]}, \quad (1)$$

$$r_a = \frac{1}{ku_*} \left[\ln\left(\frac{z_a}{z_{oH}}\right) - \psi_H\left(\frac{z_a}{L}\right) + \psi_H\left(\frac{z_{oH}}{L}\right) \right], \quad (2)$$

and

$$Q_H = \frac{(X - Y)(A - B) + C}{X + Z(X - Y)}, \quad (3)$$

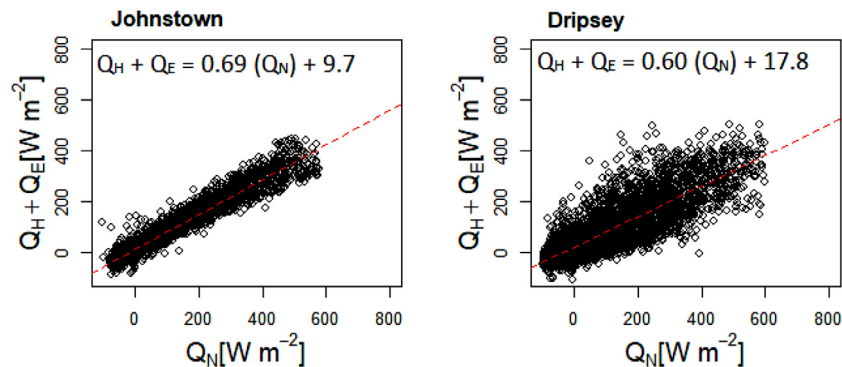


Fig. 2. The hourly Surface energy balance closure at both sites.

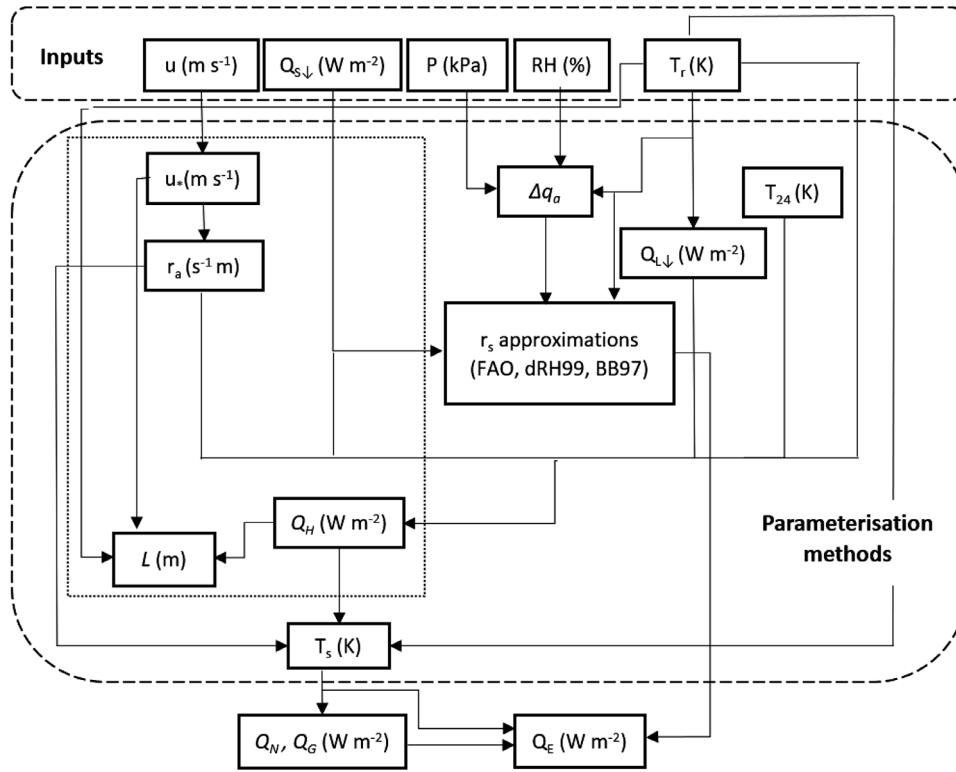


Fig 3. Schematic diagram of surface energy balance estimates. The dotted line denotes the iteration process using MOST, while the dashed lines show the input and output variables and parameterization workflow.

where

$$X = (s + \gamma) \left[s + \gamma \left(1 + \frac{r_s}{r_a} \right) \right], \quad (3a)$$

$$Y = s(s + \gamma), \quad (3b)$$

$$A = (1 - \alpha)Q_{s\downarrow} + Q_{L\downarrow} + 3\varepsilon\sigma T_a^4 + A_g T_{24}, \quad (3c)$$

$$B = (4\varepsilon\sigma T_a^3 + A_g)(T_a + z_a \Gamma_d), \quad (3d)$$

$$C = -(s + \gamma), \quad (3e)$$

$$Z = (4\varepsilon\sigma T_a^3 + A_g)(r_a/\rho c_p), \quad (3f)$$

where, ψ_H and ψ_m are the dimensionless stability correction terms for heat and momentum, respectively (Beljaars and Holtslag, 1991). The specified dimensionless constants include the surface albedo, $\alpha = 0.23$, and surface emissivity, $\varepsilon = 0.94$. We employed the following empirical values: $A_g = 9.0 \text{ W m}^{-2} \text{ K}^{-1}$, Stefan Boltzmann's constant (σ) = $5.67 \times 10^{-8} \text{ W m}^{-2} \text{ K}^{-1}$, observation height $z_a = 2 \text{ m}$, dry adiabatic lapse rate $\Gamma_d = 0.01 \text{ K m}^{-1}$, air density $\rho = 1.225 \text{ kg m}^{-3}$, specific heat capacity of air $c_p = 1005 \text{ J kg}^{-1} \text{ K}^{-1}$, von Kármán constant $k = 0.41$, surface roughness length for heat $z_{oH} = 0.001 \text{ m}$ and momentum $z_{om} = 0.01 \text{ m}$ (Table 3). The incoming longwave radiation $Q_{L\downarrow}$ (W m^{-2}) is estimated using the formulations described in the Appendix.

Initially, the iterative procedure makes a first guess of u_* , r_a and subsequently Q_H , assuming neutral stability conditions ($1/L = 0$). Using this initial estimate of Q_H , the parameters θ_* and L are calculated (see Appendix 3). This procedure is repeated until the Q_H values from one iteration to the next change by $\leq 10^{-5} \text{ W m}^{-2}$, achieved through the stability correction terms and based on the level of agreement between the estimated and measured values. The estimated Q_H (W m^{-2}) is then used to sequentially derive surface temperature T_s (K), which in turn is used to estimate Q_G (W m^{-2}) and Q_N (W m^{-2}), as follows:

$$T_s = T_a + \frac{Q_H r_a}{\rho c_p} + z_a \Gamma_d, \quad (4)$$

$$Q_G = A_g (T_s - T_{24}), \quad (5)$$

$$Q_N = [(1 - \alpha)Q_{s\downarrow} + (\varepsilon_a - 1)(\varepsilon_a \sigma T_a^4)] - [4\varepsilon\sigma T_a^3(T_s - T_a)], \quad (6)$$

where ε_a is the apparent atmospheric emissivity (see Appendix).

Finally, Q_E (W m^{-2}) is computed using the Penman Monteith formulation (Monteith, 1981), as follows,

$$Q_E = \frac{r_a s (Q_N - Q_G) + \rho c_p (e_s - e_a)}{(s + \gamma) r_a + \gamma r_s} \quad (7)$$

The turbulent fluxes (Q_H and Q_E) both rely on surface resistance (r_s) which represents the role of environmental factors, such as plant growth and soil moisture availability in regulating the surface-air exchange of water vapor.

2.4.2. Surface resistance (r_s)

There are several formulations in the literature for estimating appropriate values for r_s for different land-cover and environmental conditions. The simplest of these is the FAO value which is constant and based on a grass reference crop height of 0.12 m (Allen et al., 1998), that is

Table 3

Surface input parameters and corresponding values used at the selected stations.

Surface parameter	Value
Emissivity, ε	0.94
Albedo, α	0.23
Soil heat transfer coefficient, A_g	$9 \text{ W m}^{-2} \text{ K}^{-1}$
Roughness length for heat, z_{oH}	0.001 m
Roughness length for momentum, z_{om}	0.01 m
Surface resistance, r_s	with approximations

$$r_s = 70 \text{ s m}^{-1} \quad (8)$$

A more physically-based formulation was proposed by de Rooy and Holtslag (1999) based on a statistical relationship between r_s and the vapor density deficit (Δq) in the overlying air,

$$r_s = a + b \frac{e_s - e_a}{p} \frac{R_d}{R_v} = 10 \Delta q, \quad (9)$$

where, a (0 s m^{-1}) and b ($10 \text{ s kg m}^{-1} \text{ g}^{-1}$) are empirical constants and p is pressure such that $\frac{e_s - e_a}{p}$ is dimensionless. The remaining terms are constants, R_d is specific gas constant for dry air ($287 \text{ J kg}^{-1} \text{ K}^{-1}$) and R_v is specific gas constant for water vapor ($462 \text{ J kg}^{-1} \text{ K}^{-1}$).

Jarvis (1976) proposed a formulation for stomatal conductance, the inverse of surface resistance, that accounts for plant growth through the inclusion of environmental factors and a minimum surface resistance ($r_{s, \min}$), specific to plant type and leaf area index (LAI),

$$r_s = \frac{r_{s, \min}}{\text{LAI}} F_S F_{\Delta q} F_T F_M, \quad (10)$$

where $r_{s, \min}$ represents the optimum conditions for evapotranspiration as a function of solar radiation (F_S), water vapor ($F_{\Delta q}$), air temperature (F_T) and soil moisture (F_M) (Jarvis, 1976; Stewart, 1988). For short grass, the value of $r_{s, \min}$ is 110 s m^{-1} . Although the LAI of short grass changes seasonally (van den Hurk et al., 2000), a fixed value of $2 \text{ m}^2 \text{ m}^{-2}$ is commonly used (e.g. Beljaars and Bosveld, 1997; de Rooy and Holtslag, 1999; van den Hurk et al., 2000; 2003; van de Boer et al., 2014a).

Beljaars and Bosveld (1997) modified the Jarvis–Stewart approximation by removing the air temperature term (F_T), due to its correlation with radiation, and included a scaling factor (f_r), to adjust r_s to a particular surface (van de Boer et al., 2014a), as follows, (Beljaars and Bosveld, 1997).

$$r_s = f_r \frac{r_{s, \min}}{\text{LAI}} F_S^{-1} F_{\Delta q}^{-1} F_M^{-1} \quad (11)$$

Based on observations over the Cabauw grassland site which has poorly drained soils, Beljaars and Bosveld (1997) derived an optimized value for f_r of 0.47. Values for $r_{s, \min}$ and LAI are as stated above.

The response function F_S to $Q_{s\downarrow}$ is described (following Beljaars and Bosveld, 1997; van de Boer et al., 2014a) as:

$$F_S = \frac{Q_{s\downarrow} (S_{rm} - S_r)}{S_{rm} Q_{s\downarrow} + S_r (S_{rm} - 2Q_{s\downarrow})}, \quad (11a)$$

where the empirical coefficients S_{rm} and S_r are given as 1000 W m^{-2} and 230 W m^{-2} , respectively.

The response function $F_{\Delta q}$ to atmospheric moisture deficit is calculated as,

$$F_{\Delta q} = \frac{1}{(1 + h_s \Delta q)}, \quad (11b)$$

where Δq is the difference between the water vapor deficit at the

reference height (2 m) and surface (Chen and Dudhia, 2001). Following Beljaars and Bosveld (1997) and van de Boer et al. (2014a) we adopt a fixed value of 3 g kg^{-1} for the vapor deficit at the surface. Different values of h_s have been adopted in the literature (e.g. Stewart and Gay, 1989; Chen et al., 1996; van den Hurk et al., 2000; Chen and Dudhia, 2001, Ronda et al., 2001), however, 0.16 kg g^{-1} is employed here as it has previously been used over grassland land cover (Beljaars and Bosveld, 1997; van de Boer et al., 2014a).

F_M is a soil moisture response function and is given as,

$$F_M = 1 \text{ for } \theta > \theta_{FC}, \quad (11c)$$

$$F_M = 1 + c_{soil} (\theta - \theta_{FC}) \text{ for } \theta < \theta_{FC}, \quad (11d)$$

where θ ($\text{m}^3 \text{ m}^{-3}$) is the volumetric soil moisture in the root zone and θ_{FC} ($\text{m}^3 \text{ m}^{-3}$) is the volumetric water content at field capacity specific to soil type (Table 1). We initially employ a value of $6.3 \text{ m}^3 \text{ m}^{-3}$ for c_{soil} (following Beljaars and Bosveld, 1997); this parameter alters the relationship (i.e. slope) between conductance and soil moisture and consequently the sensitivity of F_M to changes in soil moisture.

2.4.3. Simulating fluxes at the test sites

To address our three primary objectives, here we evaluate the de Rooy and Holtslag (1999) scheme against the measured fluxes at the Johnstown Castle and Dripsey grassland sites. In particular, we focus on the different formulations for surface resistance (r_s) and their ability to estimate surface fluxes at i) a site that exhibits similar soil moisture properties to the Cabauw site, over which the scheme was originally developed, and ii) a site with differing soil moisture properties.

In the following section we use abbreviations to represent the different formulations used to obtain r_s :

- 1 FAO to identify r_s obtained using Eq. (8)
- 2 dRH99 to identify r_s obtained using Eq. (9) and,
- 3 BB97 to identify r_s obtained using Eq. (11)

The analysis is carried out for daytime only ($Q_{s\downarrow} > 10 \text{ W m}^{-2}$) when the majority of evapotranspiration takes place. At Johnstown Castle, we employ data from the nearby meteorological station and θ from the Eddy-covariance flux site as input to the scheme. At Dripsey, we employ data from Cork Airport, which is 25 km distant and is the closest suitable meteorological station. Due to the absence of soil moisture measurements for the period of study, we employ soil moisture data from 2005 as a surrogate to test the BB97 formulation in estimating r_s and Q_E at this site. We justify this on the basis that the cumulative precipitation during 2005, when the volumetric water content measurements are available, and 2010, when the flux measurements were obtained, display a similar profile during the period when soil moisture is likely to be most influential. Section 3.1 presents the results of the analysis.

Beljaars and Bosveld (1997) derived values for the f_r , S_r , h_s and c_{soil} coefficients employed in BB97 based on their model fit to the measured

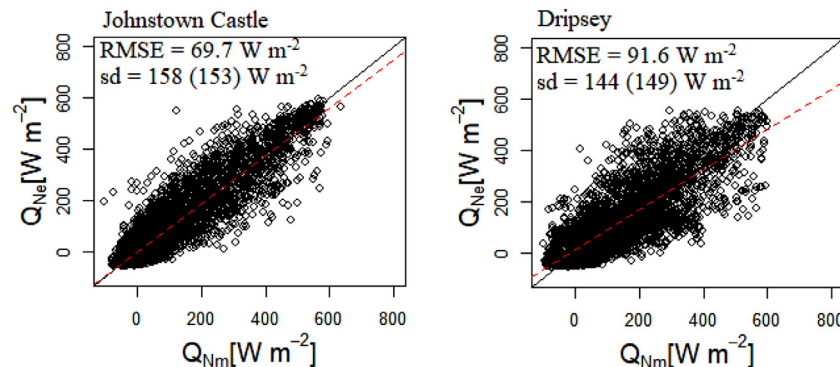


Fig 4. Relationship between daytime hourly measured (Q_{Nm}) and estimated (Q_{Ne}) net radiation flux over both sites.

data at Cabauw. To assess the influence of these specified values on r_s and consequently Q_E at both sites, we undertook a local sensitivity analysis, employing a one-at-a-time technique. For each coefficient value altered, the remaining values are held at their original, specified values. We initially perturbed the values of f_r , S_r , h_s and c_{soil} at Johnstown Castle, where all the required measured input variables are available. For consistency and robustness of model evaluation, we conducted a similar sensitivity analysis for the Dripsey site, employing soil moisture data from 2005. Finally, we employ the optimized values derived from the sensitivity analysis to derive estimated Q_H and Q_E at Johnstown Castle, where the default values for BB97 failed to replicate the measured fluxes; results from the sensitivity analysis are presented in Section 3.2.

3. Results

The de Rooy and Holtslag (1999) scheme is used, with different approximations of r_s , to simulate hourly radiation and turbulent fluxes at each observation site. The estimated hourly Q_N , Q_H and Q_E and daily averaged Q_H and Q_E fluxes were compared with the observed fluxes at each site using a number of statistical measures including root mean square error (RMSE), bias, standard deviation (sd) and correlation coefficient (r), and results are presented below.

3.1. Evaluation of radiation and estimated surface fluxes

3.1.1. Net radiation

Fig. 4 shows the relationship between estimated and measured (daytime) hourly Q_N values for both sites. The estimated (measured) Q_N values are: between -90 and 600 $W\ m^{-2}$ (-100 and 635 $W\ m^{-2}$) at Johnstown Castle and; between -66 and 553 $W\ m^{-2}$ (-100 and 600 $W\ m^{-2}$) at Dripsey. At Johnstown Castle, the model tended to overestimate negative values of Q_N and underestimate large positive values. At Dripsey, the underestimation of Q_N is likely attributable to its reliance on Q_{S1} which was derived based on hourly sun duration obtained from a distant meteorological site. Overall model performance at the two sites indicates: a $RMSE = 69.7$ $W\ m^{-2}$ ($sd = 158$ and 153 $W\ m^{-2}$ for the estimated and measured values, respectively) at Johnstown Castle and; a $RMSE = 91.6$ $W\ m^{-2}$ ($sd = 144$ and 149 $W\ m^{-2}$ for the estimated and measured values) at Dripsey. These results are broadly comparable with other similar studies. For example, Holtslag and van Ulden (1983) derived a linear relationship between Q_{S1} , solar elevation and total cloud cover, in combination with other components of the surface radiation budget, to estimate Q_N under both clear and cloudy sky conditions at Cabauw and obtained a $RMSE$ of 63 $W\ m^{-2}$ for Q_N under all conditions.

3.1.2. Sensible heat fluxes

Table 4 shows the performance metrics for the estimated hourly Q_H for both sites using the three formulations for r_s outlined above. Of these, dRH99 was found to perform the best across all metrics and both sites, but particularly at Johnstown Castle, displaying the lowest RMSE and bias and highest r values. BB97 performs the poorest at Johnstown Castle, displaying the highest RMSE and bias compared to the other two methods. In contrast, at Dripsey, BB97 produces metrics that are very similar to dRH99.

Figs. 5 and 6 display the scatterplots of measured and estimated hourly Q_H , using the three formulations of r_s , at Johnstown Castle and Dripsey, respectively; they also show the daily cycle of Q_H , during daylight hours, averaged for the month of July for the respective year of observation. At Johnstown Castle, BB97 significantly overestimates Q_H (which is evident in the July graph) while both dRH99 and FAO match the measured values more closely (Fig. 5). In general, large positive hourly values of Q_H are underestimated at Dripsey but daytime values during July are very close (Fig. 6). Of the three r_s methods, dRH99, at both sites, and BB97, at Dripsey, produced results that are most

comparable with Holtslag and van Ulden (1983) who employed a modified Priestly-Taylor approach to estimate Q_H and Q_E above a short-grass covered surface at Cabauw; they reported a $RMSE$ of 34 $W\ m^{-2}$ between measured and estimated Q_H .

3.1.3. Latent heat fluxes

Table 5 shows the statistics for the estimated and measured Q_E values for both sites. Although the FAO method employs a constant r_s value, it produced the best fit at Johnstown Castle ($RMSE = 34.9$ $W\ m^{-2}$, $bias = -6.7$ $W\ m^{-2}$ and $r = 0.85$) (Table 5), followed by dRH99 ($RMSE = 43.1$ $W\ m^{-2}$, $bias = 11.7$ $W\ m^{-2}$ and $r = 0.84$). Employing the default Beljaars and Bosveld (1997) values, BB97 performed very poorly at this site ($RMSE = 56.1$ $W\ m^{-2}$, $bias = -29.9$ $W\ m^{-2}$ and $r = 0.62$). At Dripsey, FAO produced the best fit in terms of RMSE and r value ($RMSE = 38.9$ $W\ m^{-2}$ and $r = 0.84$), but displayed the highest bias ($bias = -11.8$ $W\ m^{-2}$) of the three methods. dRH99 performed the poorest at this site, with the highest RMSE and lowest r value ($RMSE = 48.7$ $W\ m^{-2}$ and $r = 0.78$) relative to the other two methods. BB97 resulted in the lowest bias value of all methods ($bias = -2.1$ $W\ m^{-2}$), and an RMSE and r value comparable to FAO ($RMSE = 41.2$ $W\ m^{-2}$ and $r = 0.83$).

Figs. 7 and 8 show scatterplots of hourly measured and estimated Q_E , based on the different r_s formulations, for Johnstown Castle and Dripsey, respectively; they also shows the daily cycle of Q_E for daylight hours, averaged for the month of July. While FAO produced the lowest RMSE and bias values at Johnstown Castle (Table 5), both FAO and dRH99 are shown to overestimate Q_E , evident during the mid-day hours in July, when radiation is most intense; BB97 significantly underestimates Q_E , evident during July (Fig. 7). At Dripsey, all r_s methods underestimate Q_E , with the largest underestimates associated with FAO. Holtslag and van Ulden (1983), in their study over Cabauw, report a $RMSE$ of 56 $W\ m^{-2}$ between measured and estimated Q_E ; results for all r_s methods used here are consistent with this finding.

3.2. Surface resistance

To explore the difference in performance between the r_s formulations, we examined the calculated r_s ranges during daytime hours for both dRH99 and BB97. From Table 6, the range in r_s values are larger for BB97 than for dRH99, at both sites. The large difference in estimated r_s values between dRH99 and BB97 result in a marked contrast in the estimated Q_E values at Johnstown (Fig. 7). In contrast, the difference in the range of r_s values at Dripsey between methods is smaller; smaller differences are also apparent in the estimated Q_E between these methods at this site. To further examine this, we focus our attention on BB97 to understand the role of the environmental response factors in regulating r_s and consequently Q_E at both sites.

3.2.1. Sensitivity of Q_E to soil and environmental factors

A sensitivity analysis on BB97 was conducted by altering the values of f_r , S_r , h_s and c_{soil} , individually, and leaving the remaining coefficients unchanged.

At Johnstown, the estimated Q_E was found to be largely insensitive, within the range of values tested, to alterations in either h_s , associated

Table 4

Performance assessment of daytime ($Q_{S1} > 10$ $W\ m^{-2}$) Q_H based on different r_s , over both stations. The italicized values show the r_s method that give the best agreement between estimated and measured Q_H . RMSE and Bias ($W\ m^{-2}$).

r_s , method	Dripsey			Johnstown Castle		
	RMSE	Bias	r	RMSE	Bias	r
dRH99	38.2	9.4	0.78	36.1	8.3	0.83
BB97	39.8	11.9	0.77	51.8	23.4	0.83
FAO	44.7	16.7	0.77	43.8	15.9	0.82

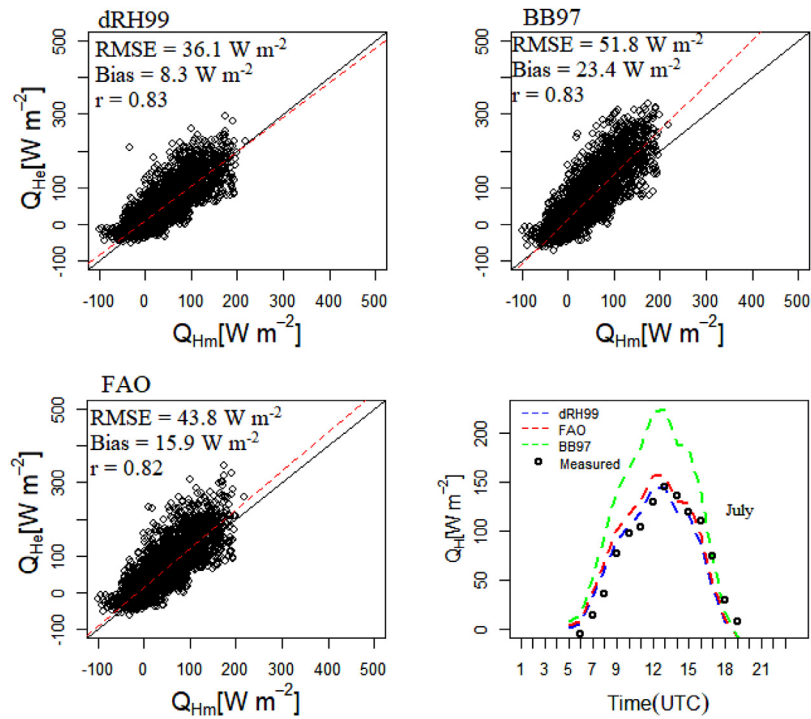


Fig 5. Relationship between daytime hourly measured (Q_{Hm}) and estimated (Q_{He}) sensible heat flux applying the Scheme with different r_s models over Johnstown Castle. The line plot is the diurnal cycle of Q_H , averaged for July, 2013.

with the atmospheric moisture deficit function ($F_{\Delta q}$), or S_r , associated with the radiation function (F_s) (Fig. 9, top) during January or July. In contrast, during July, r_s and consequently Q_E was found to be very sensitive to changes in c_{soil} , associated with the soil moisture function (F_M) (Fig. 9, bottom left). When the default value ($6.3 \text{ m}^3 \text{ m}^{-3}$) for c_{soil} was employed, the average daytime value of r_s increased significantly ($\approx 600 \text{ s m}^{-1}$), suppressing the estimated Q_E values (Fig. 7). When

$c_{soil} = 0 \text{ m}^3 \text{ m}^{-3}$, equivalent to setting $F_M = 1$, the estimated Q_E increases to near its potential, in response to low daytime r_s ($< 50 \text{ s m}^{-1}$) values. Setting c_{soil} values within the range of $2.3\text{--}4.3 \text{ m}^3 \text{ m}^{-3}$ resulted in Q_E estimates with the lowest bias, relative to measured values. A similar response was found for f_r ; estimated Q_E decreased from its potential ($f_r = 0$) with increasing f_r . A $c_{soil} = 4.3 \text{ m}^3 \text{ m}^{-3}$ was ultimately selected, based on the bias value

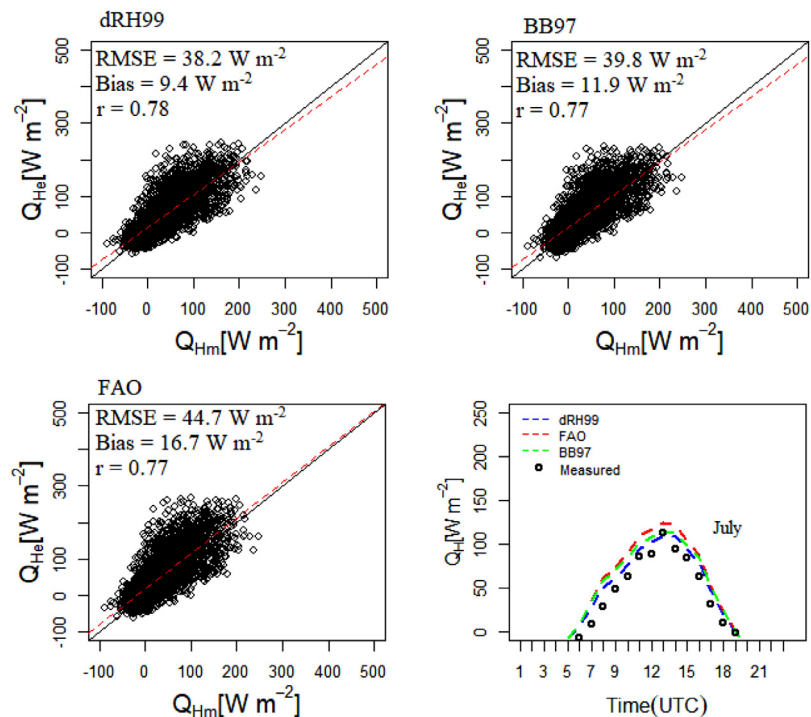


Fig 6. Relationship between daytime hourly measured (Q_{Hm}) and estimated (Q_{He}) sensible heat flux applying the Scheme with different r_s models over Dripsey. The line plot is the diurnal cycle of Q_H , averaged for July, 2010.

Table 5

Performance assessment of daytime ($Q_{s_i} > 10 \text{ W m}^{-2}$) Q_E based on different r_s , over both stations. The italicized values show the r_s method that give the best agreement between estimated and measured Q_E . RMSE and Bias (Wm^{-2}).

r_s method	Dripsey			Johnstown Castle		
	RMSE	Bias	<i>r</i>	RMSE	Bias	<i>r</i>
dRH99	48.7	5.6	0.78	43.1	11.7	0.84
BB97	<i>41.2</i>	<i>-2.1</i>	<i>0.83</i>	56.1	-29.9	0.62
FAO	38.9	-11.8	0.84	<i>34.9</i>	<i>-6.7</i>	<i>0.85</i>

(0.9 W m^{-2}) for the month of July.

At Dripsey, changes to h_s , S_r and c_{soil} had little or no impact on r_s and consequently Q_E (Fig. 10, top and bottom left), during either January or July. Similar to the findings at Johnstown, r_s was found to increase with increasing f_r so that the corresponding Q_E decreases, evident during the mid-day hours in both January and July.

3.2.2. Estimation of surface fluxes using adjusted coefficients

Fig. 11 (top) shows the hourly measured and estimated fluxes of Q_E and Q_H and averaged hourly day time values for July (Fig. 11, bottom). The use of adjusted values (Table 7) at Johnstown improves the RMSE and bias for Q_E ($RMSE = 37.8 \text{ W m}^{-2}$, $bias = -9.7 \text{ W m}^{-2}$) and Q_H ($RMSE = 41.7 \text{ W m}^{-2}$, $bias = 15.3 \text{ W m}^{-2}$) and the r value for Q_E ($r = 0.82$). The diurnal cycle (Fig. 11, bottom) shows clearly that Q_E is significantly improved, matching more closely with the measured values during July. Overall, the magnitudes of daytime hourly estimated (measured) Q_H were within the range -60 and 320 W m^{-2} (-100 and 220 W m^{-2}), while that of Q_E were within -100 and 350 W m^{-2} (-20 and 310 W m^{-2}). At Dripsey, using the original BB97 values which proved to be optimum for this site, the surface fluxes were estimated within the range -68 and 235 W m^{-2} for Q_H and within -11 and 330 W m^{-2} for Q_E .

Averaged daily Q_H were estimated between -50 W m^{-2} and 170 W m^{-2} at both sites; daily Q_E values ranged between -15 W m^{-2}

and 190 W m^{-2} at both sites (Fig. 12, top). While both sites showed similar exchanges of Q_H , at both hourly and daily time scales Q_E was higher than Q_H . This indicates that the surface conditions at these sites were wet, in general, resulting in lower Δq_a and r_s and consequently, higher Q_E . The broader pattern shows the seasonal variation in the fluxes, which are low in winter and peak in summer (Fig.12, bottom).

4. Discussion

4.1. Physical control of parameterized surface resistance and surface fluxes

In this study, we evaluated the land surface parameterization scheme of de Rooy and Holtslag (1999) as a means of deriving surface energy fluxes using routine meteorological data. Although the scheme was developed using observations made over short grass grown on poorly drained soil, they suggested it could be adjusted for use elsewhere if the surface parameters, particularly surface resistance (r_s), are modified to local conditions by using appropriate parameterization schemes. Beljaars and Bosveld (1997) indicate that r_s can vary owing to a range of environmental factors, including soil moisture, photosynthetically active radiation (PAR) and near-surface moisture deficit. Here, we focus on three different methods (namely FAO, dRH99 and BB97) of representing r_s , representing varying levels of sophistication, within the scheme.

The FAO method requires no information on atmospheric and site conditions and assigns a fixed value for r_s . Estimates using this method performed relatively well in estimating Q_E but poorly in estimating Q_H at both sites. The dRH99 method incorporates the near-surface moisture deficit but did not perform as well as FAO for Q_E , but did better than FAO for Q_H at both sites. The most sophisticated method (BB97), using the standard values for the environmental response factors (i.e. f_r , S_r , h_s and c_{soil}), provided a good fit to both Q_H and Q_E at Dripsey but performed poorest of all methods at Johnstown.

These results may seem counterintuitive, as the FAO method with the least information performs well, relative to the other methods with regard to Q_E . In part this can be explained by the constrained nature of

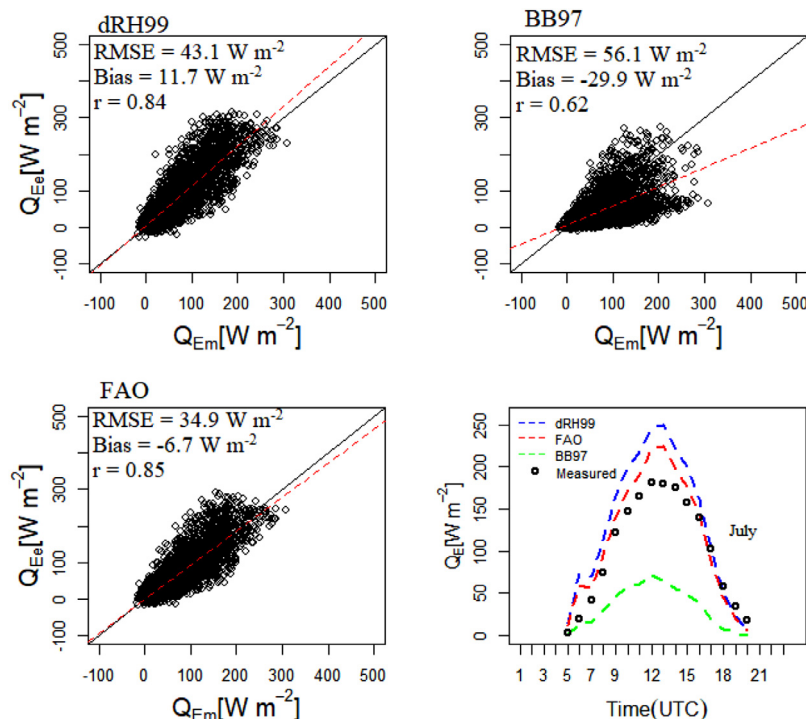


Fig 7. Relationship between daytime hourly measured (Q_{Em}) and estimated (Q_{Ee}) latent heat flux applying the Scheme with different r_s models over Johnstown Castle. The line plot is the diurnal cycle of Q_E , averaged for July, 2013.

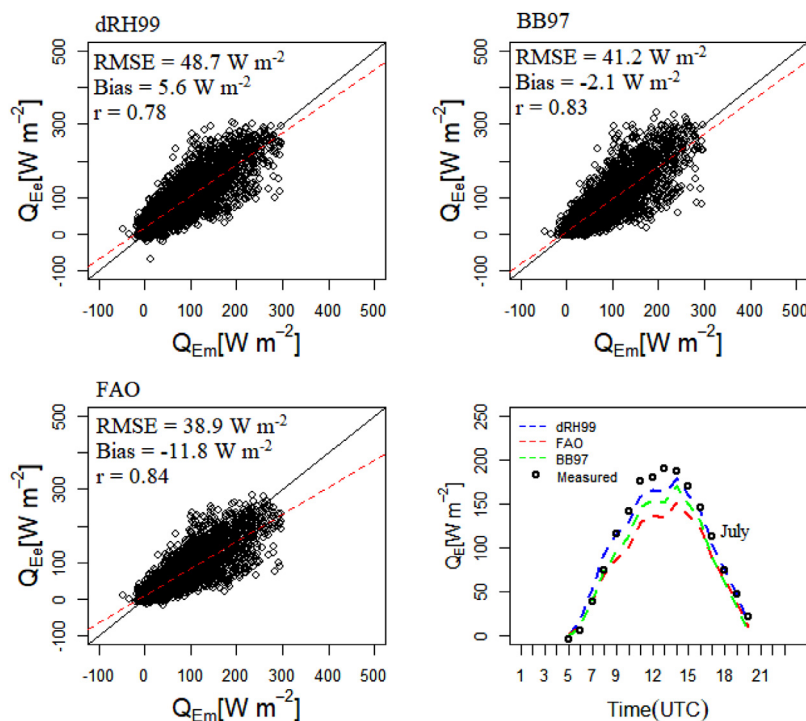


Fig 8. Relationship between daytime hourly measured (Q_{Em}) and estimated (Q_{Ee}) latent heat flux applying the Scheme with different r_s models over Dripsey. The line plot is the diurnal cycle of Q_E , averaged for July, 2010.

Table 6

Range of estimated r_s ($s m^{-1}$) during mid-day time ($Q_{S1} > 10 W m^{-2}$ and $Q_{S1} > 100 W m^{-2}$) over the selected stations. BB97 is based on the scheme using the default parameter values (i.e. Beljaars and Bosveld, 1997) for BB97; BB97 (optimized) is based on the updated optimized values for Johnstown Castle, employed in this study.

r_s method	Johnstown Castle		Dripsey	
	$Q_{S1} > 10 W m^{-2}$	$Q_{S1} > 100 W m^{-2}$	$Q_{S1} > 10 W m^{-2}$	$Q_{S1} > 100 W m^{-2}$
dRH99	0–100	0–100	0–90	0–90
BB97	25–15800	25–2613	25–1300	25–175
BB97 (optimized)	25–2450	20–400	–	–

the energy budget, which allocates the energy available (that is, $Q_N - Q_G$) into Q_H and Q_E . As FAO underestimates Q_H , more energy is channeled into Q_E . Similarly the improved performance of dRH99 for Q_H results in a weaker result for Q_E . However, the intriguing result is for the most sophisticated method (BB97), which includes many of the physical controls on r_s , performs well at Dripsey using standard values but poorly at Johnstown for both Q_H and Q_E . As both Johnstown Castle and Dripsey experience similar meteorological conditions (e.g. Fig. 4), we hypothesized that this is due to the soil moisture characteristics (Table 1), which are not considered by dRH99.

Fig. 13 shows the average daily values of soil moisture (θ) of Dripsey and Johnstown for the years available. Seneviratne et al. (2010) classified evapotranspiration regimes into types. A wet regime is defined as energy-limited, and occurs when θ lies above a critical soil moisture level (θ_{CT}). When θ falls below θ_{CT} (typically between 0.5 and 0.8 of θ_{FC}) (Seneviratne et al. 2010; after Shuttleworth, 1993) the regime is classed as moisture-limited and 'transitional'. At Dripsey, daily θ varies between 0.25 to 0.4 $m^3 m^{-3}$ over the two year period and only drops below θ_{FC} for short periods; from the 6th June to the 8th August during 2004 (≈ 64 days) and from the 28th June to the 23rd July during 2005 (≈ 26 days). At Johnstown, θ varies between 0.12 to 0.47 $m^3 m^{-3}$ over the measurement period;

however, θ falls below θ_{CT} for an extended period from the 23rd May to the 30th September during 2013 (≈ 131 days). Consistent with the soil drainage characteristics, the heavier soils at Dripsey maintain sufficient moisture throughout the year; this meets the definition of a wet regime where Q_E is constrained by the available energy. At Johnstown, in the absence of precipitation, the soil moves from a wet to a transitional regime and Q_E becomes moisture-limited. This suggests that the impact of the different methods for obtaining r_s values will be most evident during transitional soil moisture regimes. BB97 is the only method that can incorporate these effects into the calculation of surface resistance (r_s).

The sensitivity analysis identified the c_{soil} coefficient, which acts to modify the plants ability to access soil moisture below field capacity (θ_{FC}) as a critical variable. A value of $c_{soil} \approx 6.3 m^3 m^{-3}$ was estimated by Beljaars and Bosveld (1997) based on observations at a poorly-drained site (Cabauw), similar to the Dripsey site, which fits the characteristics of an energy-limited evapotranspiration regime. However, we found that a value of $c_{soil} \approx 4.3 m^3 m^{-3}$ was better suited to the imperfectly-drained soils at Johnstown, which often experiences a transitional regime. The adjusted c_{soil} value reduced the range of r_s values (Table 6) and improved results for both hourly and daily Q_H and Q_E estimates (Figs. 11 and 12). These results indicate that r_s depends very strongly on soil moisture regimes, particularly during a transitional period where θ falls below θ_{CT} , so that the use of a constant value or a linear relation where air moisture response is the only driver of r_s may prove inferior. This supports the conclusion of Beljaars and Bosveld (1997), who established that all the environmental response parameters are important for stomatal control during dry periods, in order to obtain a good flux simulation.

The estimates of surface energy fluxes generated by the de Rooy and Holtslag (1999) scheme using the BB97 method that adjusts to soil moisture conditions, generates both hourly ($RMSE \approx 40 W m^{-2}$) and daily ($RMSE \approx 24 W m^{-2}$) statistics that are comparable with other similar studies. For instance, Holtslag and van Ulden (1983), using calculated Q_{S1} as an input into their scheme, obtained half-hourly measures of $RMSE \approx 34 W m^{-2}$ for Q_H during daytime over grassland

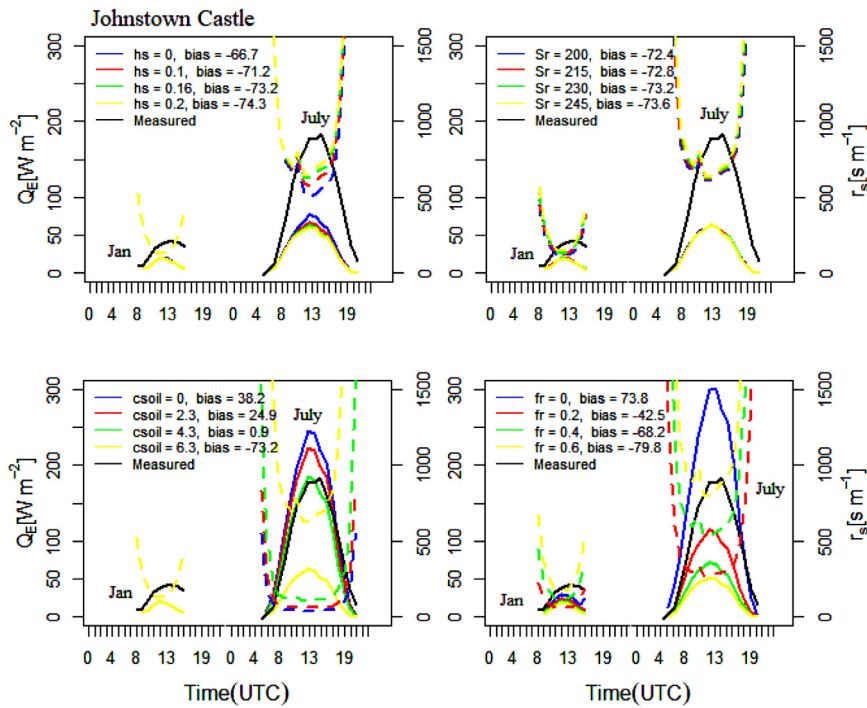


Fig 9. Sensitivity of daytime r_s and Q_E to environmental factors, averaged for January and July over Johnstown Castle. h_s (g kg^{-1}), S_r (W m^{-2}), c_{soil} ($\text{m}^3 \text{m}^{-3}$) and f_r is dimensionless. The calculated biases for January ($\approx -14 \text{ W m}^{-2}$) are similar for all factors. The dashed and solid lines are r_s and Q_E , respectively.

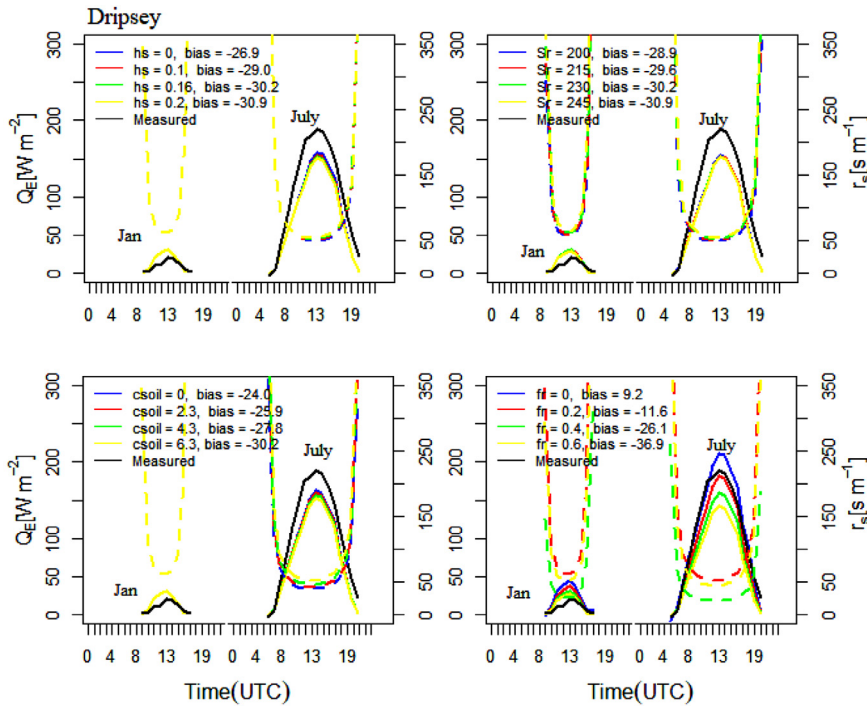


Fig 10. Sensitivity of daytime r_s and Q_E to environmental factors, averaged for January and July over Dripsey. h_s (g kg^{-1}), S_r (W m^{-2}), c_{soil} ($\text{m}^3 \text{m}^{-3}$) and f_r is dimensionless. The calculated biases for January ($\approx -9 \text{ W m}^{-2}$) are similar for all factors. The dashed and solid lines are r_s and Q_E , respectively.

at Cabauw, the Netherlands. The errors of estimated Q_E using different spatial evapotranspiration (ET) models including mapping ET at high resolution with internalized calibration (METRIC) (Allen et al., 2007), surface energy balance systems (SEBS) model (Su, 2002), two-source energy balance (TSEB) model (Norman et al., 1995), triangle model, and surface energy balance algorithm for land (SEBAL) (Bastiaanssen et al., 1998) are within the range $\approx 30\text{--}80 \text{ W m}^{-2}$ (Long and Singh, 2013), which also correspond to results in this study.

Estimated daily ET fluxes using an upscaled evaporative fraction (EF) scheme have also been found to range between 5 and 40 W m^{-2} (Colaizzi et al., 2006; Sobrino et al., 2007; Tang et al., 2013).

4.2. Uncertainties in surface heat flux simulations

It is important to recognize several potential sources of error in this work and their likely effect on the findings.

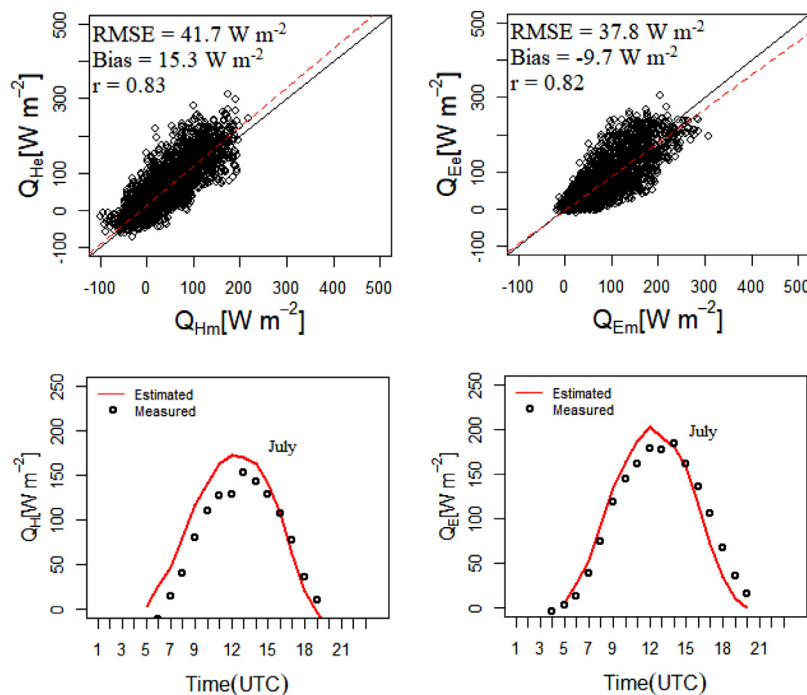


Fig 11. Relationship between daytime hourly measured and estimated Q_H [left] and Q_E [right] fluxes for 2013, applying the Scheme with optimized ($c_{soil} = 4.3 \text{ m}^3 \text{ m}^{-3}$) r_s over Johnstown Castle.

Table 7

Adapted empirical coefficients of optimized r_s for Q_E estimation under different surface conditions.

Soil Drainage Characteristics	Variable	Optimized value	Units
Imperfectly drained (Johnstown Castle)	f_r	0.47	-
	r_{smin}	110	s m^{-1}
	LAI	2	$\text{m}^2 \text{ m}^{-2}$
	h_s	0.16	g kg^{-1}
	c_{soil}	4.3	$\text{m}^3 \text{ m}^{-3}$
	S_r	230	W m^{-2}
Poorly drained (Dripsey)	f_r	0.47	-
	r_{smin}	110	s m^{-1}
	LAI	2	$\text{m}^2 \text{ m}^{-2}$
	h_s	0.16	g kg^{-1}
	c_{soil}	6.3	$\text{m}^3 \text{ m}^{-3}$
	S_r	230	W m^{-2}

Energy budget closure: The energy flux estimates generated here using the de Rooy and Holtslag scheme are evaluated by comparison with EC measurements made at two sites. It is important to acknowledge that there are likely to be errors in the measured fluxes that can be assessed as part of energy budget closure (see Section 2.3.1). Here, the closure is measured as $Q_N - (Q_H + Q_E)$ and the results for both sites (Fig. 2) are consistent with those reported in the previous studies (e.g. Wilson et al., 2002). The major reason for the non-closure here is the absence of substrate heat flux (Q_G) observations but there are also likely to be errors associated with the measured terms (Heusinkveld et al., 2004). EC measurements are known to underestimate the turbulent sensible (Q_H) and latent (Q_E) heat fluxes mainly because they do not capture the effects of large-scale eddies that are linked to landscape heterogeneity (Foken, 2008). We do not attempt to evaluate the magnitude of the underestimates in this work but Foken (2008) indicates that these may be between 10% and 20%. This should be borne in mind when evaluating the estimated turbulent fluxes using BB97, which employ adjusted parameters to improve the fit to observations.

Meteorological observations: The de Rooy and Holtslag (1999) scheme requires inputs on solar radiation, air temperature, humidity,

etc. to estimate fluxes. Ideally, these meteorological observations are complete and available at the site of study. This was not the case for Dripsey, where the scheme used data obtained for a site 25 km distant (Cork Airport) where observations of solar radiation (Q_{S1}) and cloud cover were not available. The study estimated Q_{S1} from sunshine hours using a modified Angstrom-model but could not account for the impact of clouds on Q_{L1} ; as a result, estimated Q_N is likely to be lowered, especially at night. This error will affect all surface energy fluxes but, given the focus on daytime evaporation, the impact is likely to be small. While the estimated Q_G values were not evaluated in this study, de Rooy and Holtslag (1999) also highlighted that, an overestimation of Q_G may result in negative bias in $Q_N - Q_G$ that is used to estimate Q_E .

Finally, we should acknowledge that the need to estimate radiation components (rather than using observations) will result in errors that will impact on the turbulent flux estimates produced by the different methods.

5. Summary and conclusion

This paper applied an existing physically-based scheme for estimating surface energy fluxes over two independent sites with contrasting soil moisture characteristics. The radiative and non-radiative components were parameterized from limited routine weather observations for daytime conditions over grass-covered surfaces at Johnstown Castle and Cork Airport in Ireland. The parameterized fluxes were further evaluated against observed EC flux measurements at Johnstown Castle and Dripsey (25 km from Cork Airport). Our main objectives are to test whether the original de Rooy and Holtslag (1999) scheme, which was derived at a grassland site in the Netherlands (Cabauw) can be transferred to other grassland sites and take into account different soil characteristics. The study focused in particular on the role of surface resistance (r_s) in regulating the daytime turbulent heat fluxes of Q_H and Q_E . Three methods of varying sophistication (FAO, dRH99 and BB97) were applied to the estimation scheme at the two test sites, which represent poorly (Dripsey) and imperfectly (Johnstown) drained soils. While BB97 and dRH99 produced a good fit to observed Q_E values at Dripsey (a site that is similar to Cabauw), the fit at Johnstown was

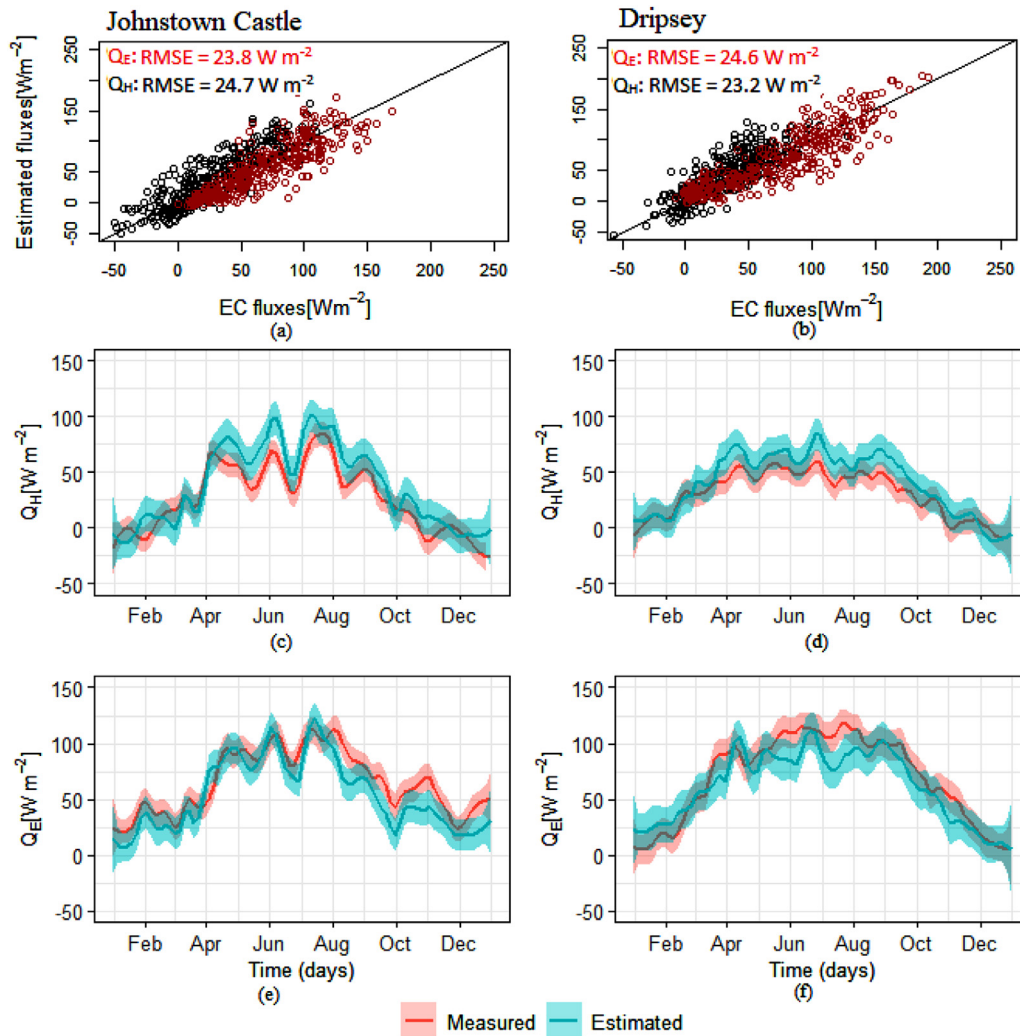


Fig 12. Relationship between parameterized and measured averaged daily Q_H and Q_E over the selected sites. The daily variations of Q_E and Q_H in the course of a year are shown in the middle (c,d) and bottom (e,f) panels, respectively. The shaded portions are the 5th and 95th percentiles of uncertainty bound as calculated by LOESS regression

poor. The differences in results were attributed to soil moisture characteristics and only BB97 accounts for this property. A critical variable in this method of deriving r_s is the soil moisture coefficient (c_{soil}), which accounts for the water available to plants for evapotranspiration; the

value of c_{soil} used in BB97 ($6.6 \text{ m}^3 \text{ m}^{-3}$) was suited to the wet soil conditions at Dripsey but not at Johnstown. This study finds that $c_{soil} \approx 4.3 \text{ m}^3 \text{ m}^{-3}$ resulted in Q_H and Q_E values that agree well with the measured values over imperfectly drained soil.

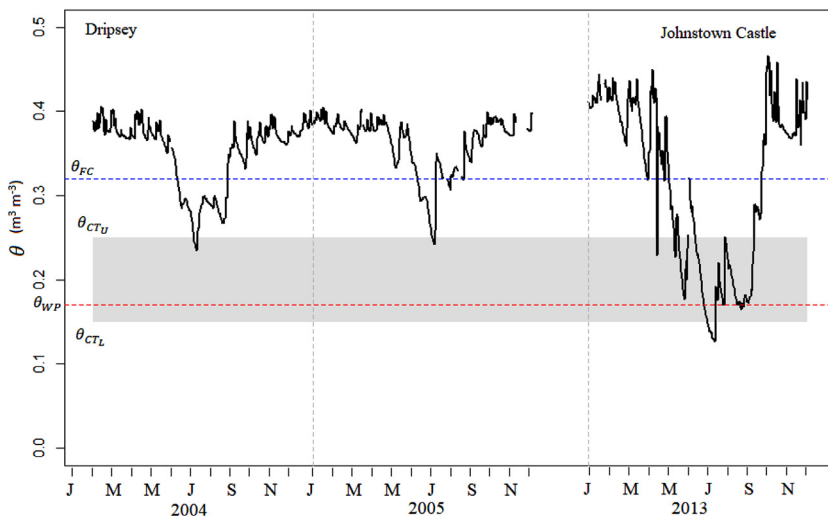


Fig 13. Averaged diurnal variations of the measured θ of the top layer of the soil from 2004 to 2005 at Dripsey and for the year 2013 at Johnstown Castle. The gaps indicate periods with missing values. The horizontal dashed line is the threshold of θ at field capacity [blue] and wilting point [red], and the grey box is the (upper and lower critical θ at $0.25 \text{ m}^3 \text{ m}^{-3}$ and $0.15 \text{ m}^3 \text{ m}^{-3}$, respectively) bound of transitional soil moisture regime for both sites (after Shuttleworth, 1993). (For interpretation of the references to color in this figure legend, the reader is referred to the web version of this article.)

An additional finding from this work was that the use of off-site meteorology, similar to the site of interest, can be reliably employed to estimate the measured surface fluxes at a location; we demonstrated this at Dripsey, where the nearest suitable meteorological station was located ≈ 25 km away. Notwithstanding the uncertainties associated the estimation of $Q_{s\downarrow}$ from sun hours and the use of soil water from a similar precipitation year (i.e. 2005), the estimated fluxes agree well with the measured values at this site. In the absence of direct soil moisture measurements and based on the soil drainage characteristics at Dripsey, the use of $F_M = 1$ in combination with standard optimal coefficients of BB97 is likely to produce similar results to dRH99.

The surface energy imbalance is always characterized to be partly a consequence of an underestimation of turbulent heat fluxes by EC techniques. Given the measures of observed surface energy balance closure at the test sites which, while they do not account for Q_G , are consistent with previous studies, we can conclude that the uncertainty of the parameterization scheme associated with the systematic bias of EC measurements of turbulent heat fluxes is relatively smaller. Notwithstanding the problems of surface energy balance closure of EC measurements, the estimated fluxes improved significantly through the adjustment of a c_{soil} adjusted to account for the soil moisture conditions. Generally, the [de Rooy and Holtslag \(1999\)](#) scheme demonstrated good performance in replicating the measured fluxes over grass-covered surfaces exhibiting different soil moisture characteristics and using routine weather observations for daytime weather conditions at both

sites. On the basis of the analysis conducted here, we therefore conclude that the land surface scheme is sensitive to soil types that exhibit different drainage characteristics; whether the optimized coefficient for c_{soil} in this study is more generally applicable, remains to be tested. The python code for this application is obtainable from the first author.

Declaration of Competing Interest

The authors declare that they have no known competing financial interests or personal relationships that could have appeared to influence the work reported in this paper.

Acknowledgments

The authors are grateful to Met Éireann, the Irish Meteorological Service, for providing routine weather observations. We thank the Dripsey FLUXNET site investigators for sharing the flux data used in this work. We acknowledge the help and advice of Prof. Bert Holtslag, Dr. Bert Heusinkveld and Dr. Arnold Moene. This study is funded by the Teagasc Irish Agriculture and Food Development Authority under Walsh Fellowship Programme (project: 2016076). We also thank the anonymous reviewers for their constructive comments to improving the quality of the study.

Appendix

A.1. Surface energy budget

The SEB is the energy conservation at the earth's surface. It describes the ability to partition the net radiation (Q_N) into surface sensible (Q_H) and latent (Q_E) heat exchange with the overlying atmosphere, and soil heat with the subsurface (Q_G) assuming no heat is stored or released within the canopy. The SEB equation can be written as;

$$Q_N = Q_H + Q_E + Q_G \quad (A1)$$

On a typical day, Q_N is positive during the day and increases toward mid-day when the sun is highest, at night it becomes negative. Consequently, the surface is the source of energy to the atmosphere leading to rising air temperature and humidity, and to the subsurface (raising soil temperature), during the daytime. However, during night-time, the surface serves as a sink as the energy flows in reverse order.

The non-radiative terms in (A1) are related to vertical gradients of air temperature (Q_H), humidity (Q_E) and soil temperature (Q_G) and the respective transfer properties. In the atmosphere, transfer is regulated by the near-surface airflow and stability while conductivity controls heat exchange in the soil. An expanded discussion of these components and application to the study region has been presented in [Keane and Collins \(2004\)](#).

A.2. Radiation terms

Q_N is parameterized based on the components of surface radiation as represented in equation A2.

$$Q_N = Q_{S\downarrow} - Q_{S\uparrow} + Q_{L\downarrow} - Q_{L\uparrow} \quad (A2)$$

The magnitude of $Q_{S\downarrow}$ depends on the Sun's altitude, clarity of the atmosphere and the latitude. This parameter is basically available by means of observations or model estimation ([Holtslag and van Ulden, 1983](#); [Ishola et al., 2018](#); for application to the study area). The $Q_{S\uparrow}$ is a fraction of $Q_{S\downarrow}$ reflected back to the atmosphere and is a function of the surface albedo ($\alpha = \frac{Q_{S\uparrow}}{Q_{S\downarrow}}$). A parameterization of surface albedo based on solar elevation has been investigated ([Beljaars and Bosveld, 1997](#); [de Rooy and Holtslag, 1999](#)), but for the purpose of simplicity, the recommended normal surface albedo value for short grass ($\alpha = 0.23$; [Oke, 1978](#)) is adopted in this study. The longwave terms in (A2) depend on the air (T_a) and surface (T_s) temperature and their respective emissivity.

A simple approximation of the incoming longwave radiation in relation to T_a at a reference height (1–2 m) has been reported ([Swinbank, 1963](#)). However, this simple empirical relation does not account for the influence of cloud cover thus, the adopted model in this study was that optimized by [Holtslag and van Ulden \(1983\)](#);

$$Q_{L\downarrow} = \varepsilon_a \sigma T_a^4 + c_1 \left(\frac{N}{8} \right) \quad (A3a)$$

$$\varepsilon_a = 1.2 \left(\frac{e}{T_a} \right)^{0.143} \quad (A3b)$$

c_1 is an empirical constants (60 W m^{-2}). A number of approximations have been proposed for ε_a , relating it to T_a and N ([Idso, 1981](#); [Holtslag and de Bruin, 1988](#)), and water vapor pressure (mbar) and T_a ([Brutsaert, 1982](#)). Here, we adopted the latter as shown in (A3a) for estimation of ε_a ([de Rooy and Holtslag, 1999](#)).

The estimation of $Q_{L\uparrow}$ depends primarily on the surface emissivity (ε) and T_s ,

$$Q_{L\uparrow} = \varepsilon\sigma T_s^4 + (1 - \varepsilon)Q_{L\downarrow} \quad (\text{A3c})$$

The literature indicates that, ε ranges from 0.9 – 0.95 for long to short grass (Oke, 1978) and 0.94 is used here (de Rooy and Holtslag, 1999). The T_s is critical for estimating $Q_{L\uparrow}$ and all of the non-radiative terms in the SEB and is discussed in the next section.

A.3. Surface temperature

Monin–Obukhov Similarity Theory (MOST) describes the profile relationships of scaling quantities, u_* , θ_* and L (Schayes, 1982; Berkowicz and Prahm, 1982; Holtslag and van Ulden, 1983; Manju and Sharma, 1987; Mohan and Siddiqui, 1998; de Rooy and Holtslag, 1999; van de Boer et al., 2014a). The temperature and wind speed profiles are given as,

$$\Delta\theta = \theta_a - \theta_s = \frac{\theta_*}{k} \left[\ln\left(\frac{z_a}{z_{oH}}\right) - \psi_H\left(\frac{z_a}{L}\right) + \psi_H\left(\frac{z_{oH}}{L}\right) \right] \quad (\text{A4})$$

$$u = \frac{u_*}{k} \left[\ln\left(\frac{z_a}{z_{om}}\right) - \psi_m\left(\frac{z_a}{L}\right) + \psi_m\left(\frac{z_{om}}{L}\right) \right] \quad (\text{A5})$$

In this study, the potential temperature θ_a is given, by adjusting the air temperature adiabatically for the height above the ground, as; $\theta_a = T_a + \frac{gz_a}{c_p}$ (de Rooy and Holtslag, 1999). Both z_{oH} and z_{om} (m) lengths are taken such that the downward-extrapolated profiles of (A4) produce effective temperature at the radiation level and the profiles of (A5) result in zero value for wind speed. de Rooy and Holtslag (1999) noted that for homogenous surfaces the local z_{oH} and z_{om} depend only on the local surface cover thus, the corresponding lengths used in this study are 0.01 m and 0.001 m for z_{om} and z_{oH} , respectively. ψ_H and ψ_m are the stability correction terms for heat and momentum (Beljaars and Holtslag, 1991). Using Businger-Dyer representations of similarity functions (Businger 1966, Dyer, 1967), Paulson (1970) has derived stability functions. The functions relate the fluxes of momentum and heat to their non-dimensional vertical gradients. The reader is referred to this paper for information on the derived stability functions in an unstable surface layer.

The scaling parameters in (A6) and (A7) are related with sensible heat flux Q_H and Obukhov length L (m) by;

$$\theta_* = -\frac{Q_H}{u_*\rho c_p} \quad (\text{A6})$$

$$L = \frac{u_*^2 T_a}{k\theta_* g} \quad (\text{A7})$$

The L is a dimensional height above the surface where the turbulence generated by buoyancy (heat production) equals the mechanically (shear) generated turbulence, describing a layer where stratification influence is negligible (Foken, 2006). Below this layer, shear production dominates over buoyancy. It is a parameter that helps to characterize the dynamic and thermodynamic processes within the atmospheric boundary layer and, in turn, the conditions of stability and instability of the surface layer. L is zero for neutral stratification and positive (negative) for stable (unstable) stratifications.

Estimation of scaling parameters requires the determination of the vertical gradients of wind and temperature from measurement at different levels, which are not available at typical meteorological stations where instruments are at one level (2 m above the earth's surface). Here, MOST is coupled with the radiative energy terms (described in Section 1) to solve a series of Eqs. ((A5)–(A7) and (A10)) by iteration; details are provided in de Rooy and Holtslag (1999).

The first step in the iterative procedure assumes neutral stability such that the last two terms on the right side of (A5) become zero and the initial values of u_* , Q_H and L are estimated. The procedure is repeated but with the inclusion of stability correction terms until the value of Q_H changes little ($\leq 10^{-5} \text{ W m}^{-2}$) with each subsequent iteration, which typically occurs after 5–6 steps (Mohan and Siddiqui, 1998). The resulting Q_H is then used to estimate surface temperature T_s using the relation in (A8).

$$T_s - T_a = \frac{Q_H r_a}{\rho c_p} + z_a \Gamma_d, \quad (\text{A8})$$

where r_a is the aerodynamic resistance (Section 4) and Γ_d is the dry adiabatic lapse rate (0.01 K m^{-1})

A.4. The soil heat flux

A number of relations describing the soil heat flux (Q_G) have been investigated against measured values in the literature (Nickerson and Smiley, 1975; Deardorff, 1978; Schayes, 1982; de Rooy and Holtslag, 1999; van de Boer, 2014a). de Rooy and Holtslag (1999) verified the simple approximation of Q_G proposed in van Ulden and Holtslag (1985) for short grass (A9) using the daily mean T_a ,

$$Q_G = -A_g(T_{24} - T_s) \quad (\text{A9})$$

where T_{24} is the 24-h mean of 2-m temperature (K), T_s is the estimated surface temperature (K), A_g is an empirical constant for soil heat transfer ($9 \text{ W m}^{-2} \text{ K}^{-1}$). This is the approximation used here.

A.5. The sensible and latent heat fluxes

The basic formulation of Q_H and Q_E fluxes has been simplified by the Penman–Monteith equation where the parameterized available energy ($Q_N - Q_G$) was partitioned (Monteith, 1981).

$$Q_H = \frac{r_a \gamma (Q_N - Q_G) - \rho c_p (\Delta q_a - \Delta q_s)}{(s + \gamma) r_a} \quad (A10)$$

$$Q_E = \frac{r_a s (Q_N - Q_G) + \rho c_p (\Delta q_a - \Delta q_s)}{(s + \gamma) r_a + \gamma r_s} \quad (A11)$$

The Penman–Monteith concept has been widely recommended for estimating Q_E at different locations (Allen et al., 1998).

The aerodynamic (r_a) and surface (r_s) resistances capture the atmospheric and canopy controls on the transfer of heat and moisture, respectively. The canopy can regulate the availability of soil water at the surface via stomates and distinguishes the evaporative term in the SEB. Aerodynamic resistance can be approximated using M-O similarity theory,

$$r_a = \frac{1}{k u_*} \left[\ln \left(\frac{z_a}{z_{oH}} \right) - \psi_H \left(\frac{z_a}{L} \right) + \psi_H \left(\frac{z_{oH}}{L} \right) \right] \quad (A12)$$

and is included in the iteration loop described in Section 2.

References

- Allen, R.G., Pereira, L.S., Raes, D., Smith, M., 1998. Crop Evapotranspiration. Guidelines for Computing Crop Water Requirements. FAO, Rome Irrigation and Drainage Paper No. 56.
- Allen, R.G., Tasumi, M., Trezza, R., 2007. Satellite-based energy balance for mapping evapotranspiration with internalized calibration (METRIC)—Model. *J. Irrig. Drain. Eng.* 133 (4), 380–394.
- Bastiaanssen, W.G.M., Menenti, M., Feddes, R.A., Holtslag, A.A.M., 1998. A remote sensing surface energy balance algorithm for land (SEBAL) 1. formulation. *J. Hydrol.* 212–213, 198–212.
- Beljaars, A.C.M., Holtslag, A.A.M., 1991. On flux parametrization over land surfaces for atmospheric models. *J. Appl. Meteorol.* 30, 327–341.
- Beljaars, A.C.M., Bosveld, F.C., 1997. Cabauw data for the validation of land surface parameterization schemes. *J. Clim.* 10, 1172–1193.
- Berkowicz, R., Prahm, L.P., 1982. Evaluation of the profile method for estimation of surface fluxes of momentum and heat. *Atmos. Environ.* 16, 2809–2819.
- Betts, A.K., Ball, J.H., 1995. The FIFE surface diurnal cycle climate. *J. Geophys. Res.* 100, 25679–25693.
- Betts, A.K., Ball, J.H., 1998. FIFE surface climate and site-average dataset 1987–89. *J. Atmos. Sci.* 55, 1091–1108.
- Brutsaert, W., 1982. *Evaporation into the Atmosphere: Theory, History, and Applications*. Springer, Dordrecht, the Netherlands. <https://doi.org/10.1007/978-94-017-1497-6>.
- Businger, J.A., 1966. Transfer of momentum and heat in the planetary boundary layer. In: *Proceedings of Symposium on Arctic Heat Budget and Atmospheric Circulation*. the RAND Corporation, pp. 305–331.
- Ciais, P., Reichstein, M., Viovy, N., Granier, N.A., Ogee, J., Allard, V., Buchmann, N., Aubinet, M., Bernhofer, C., Carrara, A., Chevallier, F., De Noblet, N., Friend, A., Friedlingstein, P., Grünwald, T., Heinesch, B., Kerónen, P., Knohl, A., Krinner, G., Loustau, D., Manca, G., Matteucci, G., Miglietta, F., Ourcival, J.M., Pilegaard, K., Rambal, S., Seufert, G., Soussana, J.F., Sanz, M.J., Schulze, E.D., Vesala, T., Valentini, R., 2005. Unprecedented European-level reduction in primary productivity caused by the 2003 heat and drought. *Nature* 437, 529–533.
- Chen, F., Dudhia, J., 2001. Coupling an advanced land surface–hydrology model with the Penn State–NCAR MM5 modeling system. Part I: Model implementation and sensitivity. *Mon. Weather Rev.* 129, 569–585.
- Chen, F., Mitchell, K., Schaake, J., Xue, Y., Pan, H.L., Koren, V., Duan, Q.Y., Ek, M., Betts, A., 1996. Modeling of land surface evaporation by four schemes and comparison with FIFE observations. *J. Geophys. Res.* 101, 7251–7268.
- Chen, T.H., Henderson-Sellers, A., Milly, P.C.D., Pitman, A.J., Beljaars, A.C.M., Polcher, J., Abramopoulos, F., Boone, A., Chang, S., Chen, F., Dai, Y., Desborough, C.E., Dickinson, R.E., Du Menil, L., Ek, M., Garratt, J.R., Gedney, N., Gusev, Y.M., Kim, J., Koster, R., Kowalczyk, E.A., Laval, K., Lean, J., Lettenmaier, D., Liang, X., Mahfouf, J.-F., Mengelkamp, H.-T., Mitchell, K., Nasonova, O.N., Noilhan, J., Robock, A., Rosenzweig, C., Schaake, J., Schlosser, C.A., Schulz, J.-P., Shao, Y., Shmakin, A.B., Verseghy, D.L., Wetzel, P., Wood, E.F., Xue, Y., Yang, Z.-L., Zeng, Q., 1997. Cabauw experimental results from the Project for Intercomparison of Land surface Parameterization Schemes (PILPS). *J. Clim.* 10, 1194–1215.
- Colaizzi, P.D., Evett, S.R., Howell, T.A., Tolk, J.A., 2006. Comparison of five models to scale daily evapotranspiration from one-time-of-day measurements. *Trans. ASABE* 49 (5), 1409–1417.
- Creamer, R.E., Simo, I., Reidy, Carvalho, J., Fealy, R., Hallett, S., Jones, R., Holden, A., Holden, N., Hannam, J., Massey, P., Mayr, T., McDonald, E., O'Rourke, S., Sills, P., Truckell, I., Zawadzka, J., Schulte, R.P.O., 2014. Irish Soil Information System. Synthesis Report (2007-S-CD-1-S1). EPA STRIVE Programme, Wexford.
- Deardorff, J., 1978. Efficient prediction of ground surface temperature and moisture with inclusion of a layer of vegetation. *J. Geophys. Res.* 83, 1889–1903.
- De Boeck, H.J., Dreesen, F.E., Janssens, I.A., Nijs, I., 2011. Whole-system responses of experimental plant communities to climate extremes imposed in different seasons. *New Phytologist* 189, 806–817.
- De Bruin, H.A.R., Holtslag, A.A.M., 1982. A simple parameterization of the surface fluxes of sensible and latent heat during daytime compared with the Penman–Monteith concept. *J. Appl. Meteorol.* 21, 1610–1621.
- De Bruin, H.A.R., Kohsiek, W., van den Hurk, J.J.M., 1993. A verification of some methods to determine the fluxes of momentum, sensible heat, and water vapour using standard deviation and structure parameter of scalar meteorological quantities. *Bound-Layer Meteorol.* 63, 231–257.
- De Rooy, W.C., Holtslag, A.A.M., 1999. Estimation of surface radiation and energy flux densities from single-level weather data. *J. Appl. Meteorol.* 38, 526–540.
- Dwyer, N., Walsh, S., 2012. Soil moisture. Dwyer (ed). *The Status of Ireland's Climate*. Environmental Protection Agency, Wexford, Ireland, pp. 115–117.
- Dyer, A.J., 1967. The turbulent transport of heat and water vapour in an unstable atmosphere. *Q. J. R. Meteorol. Soc.* 96, 132–137.
- Dyer, A.J., 1974. A review of flux-profile relationships. *Bound-Layer Meteorol.* 7, 363–372.
- EUROSTAT, 2015. *Land Cover Statistics*. Available Online at https://ec.europa.eu/eurostat/statistics-explained/index.php/Land_cover_statistics#Land_cover_in_the_EU_Member_States.
- Foken, T., 2006. 50 years of the Monin–Obukhov similarity theory. *Bound-Layer Meteorol.* 119, 431–447.
- Foken, T., 2008. The energy balance closure problem: an overview. *Ecol. Appl.* 18, 1351–1367. <https://doi.org/10.1890/06-0922.1>.
- Franssen, H.J.H., Stöckli, R., Lehner, I., Rotenberg, E., Seneviratne, S.I., 2010. Energy balance closure of eddy-covariance data: a multisite analysis for European FLUXNET stations. *Agric. For. Meteorol.* 150, 1553–1567. <https://doi.org/10.1016/j.agrformet.2010.08.005>.
- Gardiner, M.J., Radford, T., 1980. Soil Associations of Ireland and their land use potentials. *Soil Surv. Bull.* 36, 39–124. Available online at <https://www.teagasc.ie/media/website/environment/soil/General.pdf>.
- Haymann, N., Lukyanov, V., Tanny, J., 2019. Effects of variable fetch and footprint on surface renewal measurements of sensible and latent heat fluxes in cotton. *Agric. For. Meteorol.* 268, 63–73.
- Heusinkveld, B.G., Jacobs, A.F.G., Holtslag, A.A.M., Berkowicz, S.M., 2004. Surface energy balance closure in an arid region: role of soil heat flux. *Agric. For. Meteorol.* 122, 21–37.
- Holtslag, A.A.M., Van Ulden, A.P., 1983. A simple scheme for daytime estimates of the surface fluxes from routine weather data. *J. Clim. Appl. Meteorol.* 22, 517–529.
- Holtslag, A.A.M., De Bruin, H.A.R., 1988. Applied modeling of the nighttime surface energy balance over land. *J. Appl. Meteorol.* 27, 689–704.
- Idso, S.B., 1981. A set of equations for full spectrum and 8 to 14 μm and 10.5 to 12.5 μm thermal radiation from cloudless skies. *Water Resour. Res.* 17, 295–304.
- Ishola, K.A., Fealy, R., Mills, G., Fealy, R., Green, S., Jimenez-Casteneda, A., Adeyeri, O.E., 2018. Developing regional calibration coefficients for estimation of hourly global solar radiation in Ireland. *Int. J. Sustain. Energy* 38 (3), 297–311. <https://doi.org/10.1080/14786451.2018.1499645>.
- Jacobs, C., 1994. Direct Impact of Atmospheric CO2 Enrichment on Regional Transpiration. Wageningen Agricultural University, pp. 179.
- Jarvis, P., 1976. The interpretation of leaf water potential and stomatal conductance found in canopies in the field. *Philos. Trans. R. Soc. Lond. B* 273, 593–610.
- Jung, M., Reichstein, M., Ciais, P., Seneviratne, S.I., Sheffield, J., Goulden, M.L., Bonan, G., Cescatti, A., Chen, J., de Jeu, R., Dolman, A.J., Eugster, W., Gerten, D., Gianelle, D., Gobron, N., Heinke, J., Kimball, J., Law, B.E., Montagnani, L., Mu, Q., Mueller, B., Oleson, K., Papale, D., Richardson, A.D., Rouspard, O., Running, S., Tomelleri, E., Viovy, N., Weber, U., Williams, C., Wood, E., Zaehe, S., Zhang, K., 2010. Recent decline in the global land evapotranspiration trend due to limited moisture supply. *Nature* 467, 951–954.
- Kaimal, J., Finnigan, J., 1994. *Atmospheric Boundary Layer Flows: Their Structure and Measurement*. Oxford University Press, Oxford, UK.
- Keane, T., Collins, J.F. (Eds.), 2004. *Climate, Weather and Irish Agriculture*. AGMET, UCD, Belfield, Dublin, pp. 4.
- Kiely, G., Leahy, P., Lewis, C., Sottocornola, M., Laine, A., Koehler, A.-K., 2018. GHG Fluxes from Terrestrial Ecosystems in Ireland. Research report No. 227. EPA Research Programme, Wexford. Available online at https://www.epa.ie/pubs/reports/research/climate/Research_Report_227.pdf.
- Kim, J., Verma, S.B., 1991. Modeling canopy stomatal conductance in a temperate grassland ecosystem. *Agric. For. Meteorol.* 55, 149–166.
- Knist, S., Goergen, K., Buonomo, E., Christensen, O.B., Colette, A., Cardoso, R.M., Fealy, R., Fernandez, J., Garcia-Diez, M., Jacob, D., Kartsios, S., Katragkou, E., Mayer, S., van Meijgaard, E., Nikulin, G., Soares, P.M.M., Sobolowski, S., Szepszo, G.,

- Teichmann, C., Vautard, R., Warrach-Sagi, K., Wulfmeyer, V., Simmer, C., 2017. Land atmosphere coupling in EURO-CORDEX evaluation experiments. *J. Geophys. Res. Atmos.* 122, 79–103.
- Lathuilliere, M.J., Johnson, M.S., Donner, S.D., 2012. Water use by terrestrial ecosystems: temporal variability in rainforest and agricultural contributions to evapotranspiration in Mato Grosso. *Brazil* 7 (2), 024024.
- Li, J., Wang, Y.-P., Duan, Q., Lu, X., Pak, B., Wiltshire, A., Robertson, E., Ziehn, T., 2016. Quantification and attribution of errors in the simulated annual gross primary production and latent heat fluxes by two global land surface models. *J. Adv. Model. Earth Syst.* 8, 1270–1288.
- Long, D., Singh, V.P., 2013. Assessing the impact of end-member selection on the accuracy of satellite-based spatial variability models for actual evapotranspiration estimation. *Water Resour. Res.* 49 (5), 2601–2618.
- Lu, J., Tang, R., Tang, H., Li, Z.-L., 2014. A new parameterization scheme for estimating surface energy fluxes with continuous surface temperature, air temperature, and surface net radiation measurements. *Water Resour. Res.* 50, 1245–1259.
- Ma, N., Zhang, Y., Xu, C.-Y., Szilagyi, J., 2015. Modeling actual evapotranspiration with routine meteorological variables in the data-scarce region of the Tibetan Plateau: Comparisons and implications. *J. Geophys. Res. Biogeosci.* 120, 1638–1657.
- Manju, K., Sharma, O.P., 1987. Estimation of turbulence parameters for application in air pollution modelling. *Mausam* 38, 303–308.
- Mauder, M., Desjardins, R.L., MacPherson, I., 2007. Scale analysis of airborne flux measurements over heterogeneous terrain in a boreal ecosystem. *J. Geophys. Res.* 112, D13112.
- McDonnell, J., Lambkin, K., Fealy, R., Hennessy, D., Shalloo, L., Brophy, C., 2018. Verification and bias correction of ECMWF forecasts for Irish weather stations to evaluate their potential usefulness in grass growth modelling. *Meteorol. Appl.* 25, 292–301.
- McEniry, J., Crosson, P., Finneran, E., McGee, M., Keady, T.W.J., O'Kiely, P., 2013. How much grassland biomass is available in Ireland in excess of livestock requirements? *Irish J. Agric. Food Res.* 52, 67–80.
- Mohan, M., Siddiqui, T.A., 1998. Applied modeling of surface fluxes under different stability regimes. *J. Appl. Meteorol.* 37, 1055–1067.
- Moncrieff, J., Valentini, R., Greco, S., Seufert, G., Ciccioli, P., 1997a. Trace gas exchange over terrestrial ecosystems: methods and perspectives in micrometeorology. *J. Exp. Bot.* 48 (310), 1133–1142.
- Moncrieff, J.B., Massheder, J.M., Debruin, H., Elbers, J., Friborg, T., Heusinkveld, B., Kabat, P., Scott, S., Soegaard, H., Verhoef, A., 1997b. A system to measure surface fluxes of momentum, sensible heat, water vapour and carbon dioxide. *J. Hydrol.* 189, 589–611.
- Monteith, J., 1981. Evaporation and surface temperature. *Q. J. R. Meteorol. Soc.* 107, 1–27.
- Nickerson, E.C., Smiley, V.E., 1975. Surface energy budget parameterizations for urban scale models. *J. Appl. Meteorol.* 14, 297–300.
- Niyogi, D., Raman, S., 1997. Comparison of four different stomatal resistance schemes using FIFE data. *J. Appl. Meteorol.* 36, 903–917.
- Ní Choncuibhair, Ó., Osborne, B., Finnan, J., Lanigan, G., 2017. Comparative assessment of ecosystem C exchange in *Miscanthus* and reed canary grass during early establishment. *GCB Bioenergy* 9, 280–298. <https://doi.org/10.1111/gcb.12343>.
- Norman, J.M., Kustas, W.P., Humes, K.S., 1995. A two-source approach for estimating soil and vegetation energy fluxes in observations of directional radiometric surface temperature. *Agric. For. Meteorol.* 77, 263–293.
- Oke, T.R., 1978. *Boundary Layer Climates*. Methuen, pp. 372.
- Papale, D., Reichstein, M., Aubinet, M., Canfora, E., Bernhofer, C., Longdoz, B., Kutsch, W., Rambal, S., Valentini, R., Vesala, T., Yakir, D., 2006. Towards a standardized processing of net ecosystem exchange measured with eddy covariance technique: algorithms and uncertainty estimation. *Biogeosciences* 3, 571–583.
- Paulson, C.A., 1970. The mathematical representation of wind speed and temperature profiles in the unstable atmospheric surface layer. *J. Appl. Meteorol.* 9, 857–861.
- Peel, M.C., Finlayson, B.L., McMahon, T.A., 2007. Updated world map of the Köppen-Geiger climate classification. *Hydrol. Earth Syst. Sci.* 11, 1633–1644.
- Peichl, M., Carton, O., Kiely, G., 2012. Management and climate effects on carbon dioxide and energy exchanges in a maritime grasslands. *Agric. Ecosyst. Environ.* 158, 132–146.
- Reichstein, M., Ciais, P., Papale, D., Valentini, R., Running, S., Viovy, N., Cramer, W., Granier, A., Oge, J., Allard, V., Aubinet, M., Bernhofer, C., Buchmann, N., Carrara, A., Grünwald, T., Heimann, M., Heinesch, B., Knohl, A., Kutsch, W., Loustau, D., Manca, G., Matteucci, G., Miglietta, F., Ourcival, J., Pilegaard, K., Pumpanen, J., Rambal, S., Schaphoff, S., Seufert, G., Soussana, J., Sanz, M., Vesala, T., Zhao, M., 2007. Reduction of ecosystem productivity and respiration during the European summer 2003 climate anomaly: a joint flux tower, remote sensing and modelling analysis. *Global Change Biol.* 13, 634–651.
- Ronda, R.J., de Bruin, H.A.R., Holtslag, A.A.M., 2001. Representation of the canopy conductance in modeling the surface energy budget for low vegetation. *J. Appl. Meteorol.* 40, 1431–1444.
- Russell, G., 1980. Crop evaporation, surface resistance and soil water status. *Agric. Meteorol.* 21, 213–226.
- Schayes, G., 1982. Direct determination of diffusivity profiles from synoptic reports. *J. Atmos. Sci.* 27, 1122–1137.
- Seneviratne, S.I., Corti, T., Davin, E.L., Hirschi, M., Jaeger, E.B., Lehner, I., Orlowsky, B., Teuling, A.J., 2010. Investigating soil moisture-climate interactions in a changing climate: a review. *Earth Sci. Rev.* 99 (3–4), 125–161.
- Sherratt, D.J., Wheeler, H.S., 1984. The use of surface resistance-soil moisture relationships in soil water budget models. *Agric. For. Meteorol.* 31, 143–157.
- Shi, Q., Liang, S., 2014. Surface-sensible and latent heat fluxes over the Tibetan Plateau from ground measurements, reanalysis, and satellite data. *Atmos. Chem. Phys.* 14, 5659–5677.
- Shuttleworth, W.J., 1993. Evaporation. In: Maidment, D.R. (Ed.), *Handbook of Hydrology*. McGraw-Hill Inc, New York, pp. 4.1–4.53.
- Sobrinho, J.A., Gomez, M., Jimenez-Muoz, J.C., Olioso, A., 2007. Application of a simple algorithm to estimate daily evapotranspiration from NOAA-AVHRR images for the Iberian Peninsula. *Remote Sens. Environ.* 110 (2), 139–148.
- Sottocornola, M., Kiely, G., 2010a. Hydro-meteorological controls on the CO₂ exchange variation in an Irish blanket bog. *Agric. For. Meteorol.* 150 (2), 287–297.
- Sottocornola, M., Kiely, G., 2010b. Energy fluxes and evaporation mechanisms in an Atlantic blanket bog in southwestern Ireland. *Water Resour. Res.* 46 (11), W11524.
- Stewart, J.B., 1988. Modeling surface conductance of pine forest. *Agric. For. Meteorol.* 43, 19–35.
- Stewart, J.B., Gay, L.W., 1989. Preliminary modeling of transpiration from FIFE site in Kansas, USA. *Agric. For. Meteorol.* 48, 305–316.
- Stoy, P.C., Mauder, M., Foken, T., Marcolla, B., Boegh, E., Ibrom, A., Arain, M.A., Arneth, A., Aurela, M., Bernhofer, C., Cescatti, A., Dellwik, E., Duce, P., Gianelle, D., van Gorsel, E., Kiely, G., Knohl, A., Margolis, H., McCaughey, H., Merbold, L., Montagnani, L., Papale, D., Reichstein, M., Saunders, M., Serrano-Ortiz, P., Sottocornola, M., Spano, D., Vaccari, F., Varlagin, A., 2013. A data-driven analysis of energy balance closure across FLUXNET research sites: the role of landscape scale heterogeneity. *Agric. For. Meteorol.* 171–172, 137–152. <https://doi.org/10.1016/j.agrformet.2012.11.004>.
- Su, Z., 2002. The Surface Energy Balance System (SEBS) for estimation of turbulent heat fluxes. *Hydrol. Earth Syst. Sci.* 6 (1), 85–99.
- Swinbank, W.C., 1963. Longwave radiation from clear skies. *Q. J. R. Meteorol. Soc.* 89, 339–448.
- Tang, R.L., Li, Z.-L., Sun, X.M., 2013. Temporal upscaling of instantaneous evapotranspiration: an intercomparison of four methods using eddy covariance measurements and MODIS data. *Remote Sens. Environ.* 138, 102–118.
- Teuling, A.J., Seneviratne, S.I., Williams, C., Troch, P.A., 2006. Observed timescales of evapotranspiration response to soil moisture. *Geophys. Res. Lett.* 33, L23403.
- Twine, T.E., Kustas, W.P., Norman, J.M., Cook, D.R., Houser, P.R., Meyers, T.P., Prueger, J.H., Starks, P.J., Wesely, M.L., 2000. Correcting eddy-covariance flux underestimates over a grassland. *Agric. For. Meteorol.* 103 (3), 279–300.
- van de Boer, A., Moene, A.F., Schu'temeyer, D., 2013. Sensitivity and uncertainty of analytical footprint models according to a combined natural tracer and ensemble approach. *Agric. Forest. Meteorol.* 169, 1–11.
- van de Boer, A., Moene, A.F., Graf, A., Simmer, C., Holtslag, A.A.M., 2014a. Estimation of the refractive index structure parameter from single-level daytime routine weather data. *Appl. Opt.* 1–20. <https://doi.org/10.1364/AO.53.005944>.
- van de Boer, A., Moene, A.F., Graf, A., Schu'temeyer, D., Simmer, C., 2014b. Detection of entrainment influences on surface-layer measurements and extension of Monin-Obukhov similarity theory. *Bound-Layer Meteorol.* 152, 19–44.
- van den Hurk, B.J.J.M., Viterbo, P., Beljaars, A.C.M. and Betts, A.K., 2000. Offline Validation of the ERA40 Surface Scheme. Technical Report ECMWF, 43 p.
- van den Hurk, B.J.J.M., Viterbo, P., Los, S.O., 2003. Impact of Leaf Area Index seasonality on the annual land surface evaporation in a global circulation model. *J. Geophys. Res.* 108 (D6), 4191.
- van Ulden, A.P., Holtslag, A.A.M., 1985. Estimation of atmospheric boundary layer parameters for diffusion applications. *J. Clim. Appl. Meteorol.* 24, 1196–1207.
- Vickers, D., Mahrt, L., 1997. Quality control and flux sampling problems for tower and aircraft data. *J. Atmos. Ocean. Technol.* 14, 512–526.
- Viterbo, P., Beljaars, A., 1995. An improved land-surface parameterization scheme in the ECMWF model and its validation. *J. Clim.* 8, 2716–2748.
- Webb, E., Pearman, G., Leuning, R., 1980. Correction of flux measurements for density effects due to heat and water-vapor transfer. *Q. J. R. Meteorol. Soc.* 106, 85–100.
- Walsh S., 2012. A Summary of Climate Averages for Ireland, 1981 – 2010. MET Eireann Climatological Note No. 14, Dublin. Available Online at <https://www.met.ie/climate-ireland/SummaryClimAvgs.pdf>.
- Wilson, K., Goldstein, A., Falge, E., Aubinet, M., Baldocchi, D., Berbigier, P., Bernhofer, C., Ceulemans, R., Dolman, H., Field, C., Grelle, A., Ibrom, A., Law, B.E., Kowalski, A., Meyers, T., Moncrieff, J., Monson, R., Oechel, W., Tenhunen, J., Valentini, R., Verma, S., 2002. Energy balance closure at FLUXNET sites. *Agric. For. Meteorol. FLUXNET 2000 Synth.* 113, 223–243. [https://doi.org/10.1016/S0168-1923\(02\)00109-0](https://doi.org/10.1016/S0168-1923(02)00109-0).
- Zhang, L., Xiao, J., Li, J., Wang, K., Lei, L., Guo, H., 2012. The 2010 spring drought reduced primary productivity in southwestern China. *Environ. Res. Lett.* 7 (4), 1748–9326.